의학박사 학위논문

간동맥화학색전술을 위한 항암제 함유 마이크로버블과 결합된 초음파 감응형 에멀젼 개발: 토끼 VX2 간종양 모델을 이용한 전임상 연구

Development and Evaluation of an Ultrasound-Triggered Microbubble Combined Transarterial Chemoembolization (TACE) Formulation on Rabbit VX2 Liver Cancer Model

2021년 8월

서울대학교 대학원
의학과 영상의학전공

이재환

A thesis of the Degree of Doctor of Philosophy in Medicine

간동맥화학색전술을 위한 항암제 함유 마이크로버블과 결합된 초음파 감응형 에멀젼 개발: 토끼 VX2 간종양 모델을 이용한 전임상 연구

Development and Evaluation of an Ultrasound-Triggered Microbubble Combined Transarterial Chemoembolization (TACE) Formulation on Rabbit VX2 Liver Cancer Model

August 2021

Department of Radiology,
Seoul National University
College of Medicine

Jae Hwan Lee

Development and Evaluation of an Ultrasound-Triggered Microbubble Combined Transarterial Chemoembolization (TACE) Formulation on Rabbit VX2 Liver Cancer Model

간동맥화학색전술을 위한 항암제 함유 마이크로버블과 결합된 초음파 감응형 에멀젼 개발: 토끼 VX2 간종양 모델을 이용한 전임상 연구

지도 교수 정 진 욱

이 논문을 의학박사 학위논문으로 제출함
2021년 4월

서울대학교 대학원
의학과 영상의학 전공
이 재 환

이재환의 의학박사 학위논문을 인준함
2021년 7월

위 원 장 _____ 윤 정 환
부위원장 _____ 정 진 욱
위 원 _____ 이 광 웅
위 원 _____ 천 호 종
위 원 _____ 김 정 훈

Abstract

Introduction: Transarterial chemoembolization (TACE) is an image-guided locoregional therapy used for the treatment of patients with primary or secondary liver cancer. However, conventional TACE formulations are rapidly dissociated due to the instability of the emulsion, resulting in insufficient local drug concentrations in the target tumor. The aim of this study was to prove the feasibility of albumin-doxorubicin nanoparticle conjugated microbubble (ADMB) for enhancing therapeutic efficiency by sonoporation under exposure to ultrasound, and to develop a novel drug delivery system composed of doxorubicin-loaded albumin nanoparticles-conjugated microbubble complex in iodized oil emulsion (DOX-NPs-MB complex in Lipiodol) to overcome these limitations and to evaluate safety and therapeutic efficacy of ultrasound-triggered TACE using this formulation.

Materials and methods: This study was comprised of two parts; the first part was for fabrication and evaluation of in-vitro characteristics of ADMB, including size distribution, drug release profile, and echogenicity. Therapeutic efficacy was assessed using rabbit VX2 tumor model. The second part was for development and in-vivo validation of DOX-NPs-MB complex in iodized oil emulsion as a new ultrasound-triggered TACE formulation.

Results: ADMB demonstrated a size distribution of 2.33 ± 1.34 μm and a doxorubicin loading efficiency of 82.7%. The echogenicity of ADMBs was sufficiently generated in the 2–9 MHz frequency range and cavitation depended on the strength of the irradiating ultrasound. DOX-NPs-MB constituting the complex retained their function as an

ultrasound contrast agent in Lipiodol. In the *in vivo* study, ultrasound-triggered TACE using DOX-NPs-MB complex in Lipiodol formulation (US+) showed a lower viable tumor portion than the conventional TACE formulation, and effectively killed cancer cells in the peripheral region of the tumor. Liver toxicity was comparable to that of conventional therapies.

Conclusion: In summary, by introducing a doxorubicin-loaded microbubble in the TACE formulation, it was possible to improve both drug delivery to the tumor with real-time monitoring, and therapeutic efficacy of TACE. This enhanced TACE formulation may provide a new means of treating liver cancer.

Keywords: Transarterial chemoembolization; Ultrasound microbubble; Sonoporation; Theragnostics; Nanomedicine; Hepatocellular carcinoma

Student number: 2010-21816

Table of Contents

List of Figures

Abbreviations

TACE: Transarterial chemoembolization; HSA: Human serum albumin; DOX-NPs: doxorubicin-loaded albumin nanoparticles; MB: microbubbles; ADMB: albumin-doxorubicin nanoparticle conjugated microbubble ; 2-IT: 2-iminothiolane hydrochloride; DSCP: 1,2-Distearoyl-sn-glycero-3-phosphocholine ; DSPE-PEG2k-NHS: 1,2-Distearoyl-sn-glycero-3-phosphoethanolamine-N-[amino(Polyethylene Glycol)2000] (Ammonium Salt); US: ultrasound; HPLC: high-performance liquid chromatography; PDMS: Polydimethylsiloxane; DAPI: 4',6-diamidino-2-phenylindole; PFA: Paraformaldehyde; BABB: Benzyl Alcohol and Benzyl Benzoate; MR: Magnetic resonance; IA: intra-arterial; VIR: volume inhibition rate; ADC: value of the apparent diffusion coefficient; TUNEL: terminal deoxynucleotidyl transferase dUTP nick-end labeling; AST: aspartate transaminase; ALT: alanine transaminase; HCS: high-content screening

Introduction

Image guided intra-arterial therapy, such as transarterial chemoembolization (TACE) provides a valuable tool for the treatment of primary or secondary liver cancer(1, 2). The goal of TACE is to selectively deliver anticancer agent-iodized oil emulsion (Lipiodol; Guerbet, Aulnay-sous-Bois, France) to the arterial supply of tumors. Infusion of emulsion results in both targeted delivery of high concentrations of anticancer drug directly to the tumor, and blocking of the terminal arteriole by Lipiodol (3). TACE has been adopted as a standard treatment option for intermediate-stage hepatocellular carcinoma (HCC) (4). However, clinical outcomes with TACE are still unsatisfactory, typically considered to be only a partial response in 15–55 % of patients, and to increase median survival from 16 to 20 months (5). One possible explanation for this poor outcome is low drug delivery efficiency to tumors (6). During the TACE procedure, a considerable proportion of the chemotherapeutic agent enters the systemic blood circulation due to instability of the emulsion, resulting in low drug delivery efficiency and systemic side effects. It has been postulated that insufficient local delivery of chemotherapeutic agents with the embolization of supply arteries, induces tumor hypoxia, resulting in neo-angiogenesis and metastasis, and is subsequently associated with poor outcomes (7, 8). Another related clinical problem is adverse drug reactions such as fatigue, weight loss, pain and nausea, induced by anticancer drugs leaking into the systemic circulation. Thus, the establishment of a new TACE drug delivery system which is capable of improved drug delivery and real-time imaging, is mandated for enhancing tumor control and reducing side effects.

In the last decade, microbubbles have been actively studied not only as ultrasound contrast agents but also for local drug delivery under exposure to ultrasound (US+) (9, 10). Theoretically, microbubbles exposed to ultrasound waves experience repeated volumetric expansion and contraction (11, 12). This oscillation propagates microstreams in blood vessels, and epithelial junctions near the microbubble become leaky. In addition, when collapsed under a strong ultrasonic exposure, the microbubble generates microjets and a shock wave. This microjet and shock wave temporarily induces pores in the cell membrane, and makes the membrane permeable to drug (the sonoporation effect) (13, 14). In our previous study, human serum albumin nanoparticles (HSA-NPs) were effectively delivered to the tumor site by sonoporation (15, 16) Microbubble-conjugated anticancer drug-loaded HSA-NPs (ADMB) enhanced the selective delivery of drugs to the tumor and led to the improvement of therapeutic efficiency, compared to the administration of pure drugs and administration without ultrasound irradiation. Nanoparticle-based drug delivery has been advantageous for improving drug loading efficiency, protection of drugs from degradation, and intracellular penetration via characteristics of the nanoparticles which allow a sustained drug release. Thus, when the ADMB complex in Lipiodol is infused intra-arterially, ADMB complex becomes localized in the vicinity of the blood vessel wall and the cavitation of microbubbles under the exposure of ultrasound generates jet-streaming and shock waves, resulting in weakness of the hepatic tumor vessel wall. Consequently, the chemotherapeutic agent encapsulating nanoparticles, which are conjugated onto the surface of microbubbles, will be delivered deeply into the tumor through the weakened blood vessel wall with the help

of the jet-stream (Figure 1) (17). Thus, improved drug delivery by cavitation of microbubbles under ultrasound irradiation can be expected. Simultaneously, the TACE procedure can be monitored in real time by ultrasound. Therefore the aim of this study was to explore the antitumor effect of the ADMB, and to develop a novel emulsion (ADMB complex in Lipiodol) for ultrasound triggered TACE (Figure 1).

Materials and Methods

Materials

1,2-Distearoyl-sn-glycero-3-phosphocholine (DSPC) and 1,2-Distearoyl-*sn*-glycero-3-phosphoethanolamine-N-[amino(Polyethylene Glycol)2000] (Ammonium Salt) (DSPE-PEG2k-NHS) were purchased from Avanti Polar Lipids, Inc. (Alabaster, USA). Human serum albumin (HSA), 2-iminothiolane hydrochloride, and 99% ethanol were purchased from Sigma-Aldrich (St. Louis, MO, USA). Doxorubicin Hydrochloride was purchased from the Il-Dong Pharmaceutical Company (Seoul, Korea) in a dry powder form. Microcatheters (Progreat 2.0-F, Terumo, Japan) were obtained from the Terumo Korea Corporation (Seoul, Korea). Rabbits were purchased from Orient Bio Co. (Seongnam, Korea). Lipiodol was purchased from Gurbet (Aulnay-sous-Bois, France). All other chemicals and solvents were prepared as analytical grade.

Synthesis of DOX-NPs

The doxorubicin-loaded human serum albumin nanoparticles were fabricated by desolvation method (18). Albumin was dissolved in distilled water at a concentration of

a 40 mg/mL and the pH was adjusted to 8–8.5, with 0.2 M NaOH. For thiolation, 2-iminothiolane hydrochloride (2-IT, 7.5 mg/mL) was added and the solution was reacted in a 25℃ shaker for 1 h. After thiolation of albumin, the solution was centrifuged twice at 4,000 rpm for 15 min using Amicon Ultra-30 KDa Centricons, to remove unreacted 2-IT. Then, doxorubicin-HCl (10 mg/mL) was added to the albumin solution. To form the nanoparticle, the ethanol was added dropwise to the doxorubicin and albumin mixture at a rate of 1 mL/min until the solution became turbid (desolvation) in a stirring state. The reaction mixture was stirred gently for 1 day. The solution was centrifuged at 13,200 rpm for 10 min and the supernatants were collected to confirm encapsulation efficiency of doxorubicin. The doxorubicin-loaded albumin nanoparticles were dispersed in contrast agent (Pamiray 250, Dongguk Pharmaceutical, Seoul, Korea). The encapsulation efficiency of doxorubicin was calculated by analyzing the quantity of unbounded doxorubicin in the supernatants after centrifugation by HPLC using following equation.

$$\mathrm{EE}(\%) = \frac{\mathrm{DOX\ \ total} - \mathrm{DOX\ \ free}}{\mathrm{DOX\ \ total}} \times 100\%$$

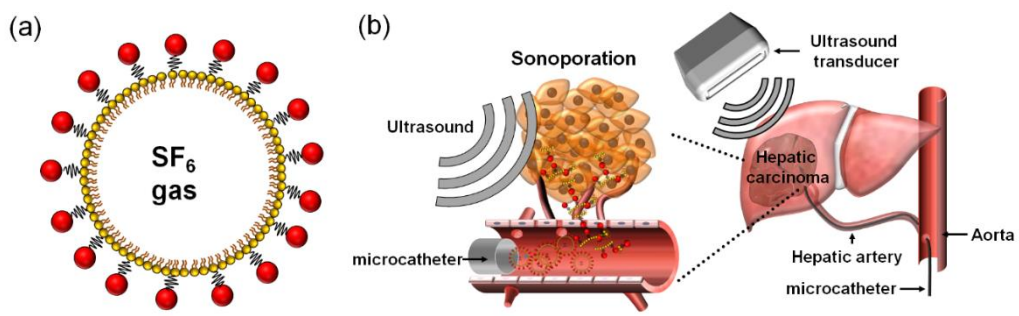

Figure 1. Schematic illustrations of (a) the IA ADMB complex and (b) treatment procedure for the intra-arterial administration of the ADMB complex using microcatheters under ultrasound exposure

Synthesis of ADMB complex

To create microbubbles, DSPE-PEG2k-NHS and DSPC were dissolved in chloroform at a molar ratio of 1:9. The chloroform was fully evaporated for fabrication of a phospholipid thin film. The phospholipid film was hydrated by PBS, pH 7.4 in 1mg/mL. The dispersed solution in the vial filled with C_3F_8 gas. Microbubbles are formed by vigorous agitation using a Vialmix™ for 45 s. Microbubbles were transferred to a 5 mL syringe and centrifuged at 1,500 rpm for 15 min to float the microbubbles. The lower part without microbubbles was discarded and upper part of the microbubbles was dispersed in a DOX-NPs solution to form DOX-NPs-MB complex. The albumin-doxorubicin nanoparticles were conjugated to the microbubbles via amide bonds between the primary amine of the nanoparticles and the NHS from the microbubble surface. The mixture of DOX-NPs and MB solution was reacted for 1 h 30 min or more in a room temperature with gentle agitation.

In-vitro release test for the ADMB complex

In order to investigate doxorubicin release from the ADMB complex, the complex was sealed with a 3000 Da (MW) cut-off dialysis membrane. The complex loaded with 1 mg of doxorubicin in the dialysis membrane was placed into the tube filled with 10 ml of phosphate buffer saline. This tube was incubated at 37 ºC and 500 rpm. The released doxorubicin was measured by a UV-Vis spectrometer.

Phantom study for echogenicity of the ADMB complex

The echogenicity of the ADMB complex was evaluated using a commercial ultrasound scanner equipped with a transducer having a frequency range of 2–9 MHz. For the ultrasound imaging, home-made agarose phantoms containing two holes of 2 cm depth was used. The holes in the agarose phantoms were filled with the ADMB complex at the concentration of 5 μg/ml and degassed water, respectively. For studying microbubble stability, ultrasound imaging was performed at a Mechanical Index (MI) of 0.06 using a manual flash of 3-second time interval for microbubble destruction. The stability of the ADMB complex was analyzed by decreasing the ratio of echogenic area with the ImageJ program.

Preparation of preclinical liver tumor model

Animal research protocols followed in this study were approved by Seoul National University of Medicine institutional animal care and use committee. Male New Zealand white rabbits (n=35) weighing 3.0–3.5 kg were used for the study. The animals were housed in cages with a 12-h light/dark cycle and ad libitum access to standard rabbit chow diet and water. During all procedures, the animals were anesthetized with intramuscular injections of 5 mg/kg body weight of tiletamine-zolazepam (Zoletil 50, Virbac, Carros, France) and a 2 mg/kg body weight of 2 % xylazine hydrochloride (Rompun; Bayer, Seoul, Korea). The VX2 carcinoma strain was maintained in the right hind limb of a carrier rabbit through deep intramuscular injection throughout the study. Briefly, the left lobe of the animal's liver was exposed surgically and a small piece of tumor tissue (1

mm^3) freshly harvested from the maintained tumor was directly implanted at the subcapsular area of the liver for each rabbit, as described in previous studies (19). The tumor was incubated for 17–18 days before treatment.

MR imaging

All animals underwent MR imaging at day 0 (baseline before treatment) and at day 7 following IA or IV infusion in the groups A to D which received treatment, and the untreated group E. A 3.0-T clinical MR scanner (TimTrio; Siemens Healthcare, Erlangen, Germany) with a knee coil was used to improve SNR and spatial resolution. The animals were fixed on a board in a supine position, and an abdominal bandage was tightly applied to reduce any movement artifact. Axial T2-weighted turbo spin-echo (repetition time/echo time: 4100 milliseconds/150 milliseconds; echo train length: 14; section thickness: 3 mm; field of view: 130 x 130 mm; matrix: 512 x 358; number of excitations: 2.0) and IVIM Diffusion-weighted image (free breathing single-shot echo-planar imaging pulse sequence with diffusion gradients applied in three orthogonal directions: 2700/63; section thickness: 3 mm; number of sections: 20; number of signals acquired: 8; field of view: 14 x 14 cm2; matrix: 128 x 128; and four b values (0, 15, 200, and 800 seconds/mm2)) were acquired [23]. The images were evaluated using a dedicated workstation for picture archiving and communication system (m-view; Marotech, Seoul, Korea).

Grouping and drug delivery

On the basis of the treatment procedure, the animals were divided into five groups having similar tumor volumes: animals receiving an intra-arterial (IA) infusion of ADMB/US

(group A, n=6), animals receiving an intravenous (IV) infusion of ADMB/US (group B, n=6), animals receiving an IA infusion of free MB/US (group C, n=5), animals receiving an IA infusion of doxorubicin/US (group D, n=3), and the untreated control (Group E, n=5). The dose of doxorubicin delivered was 1 mg for all groups except for groups C and E. In each group except the control, an infusion pump (Genie plus, Kent Scientific Corporation, Torrington, CT, USA) was used. Group A underwent an IA delivery of ADMB in 3 ml of Iopamidol (Pamiray®, Seoul, South Korea) contrast media via the proper hepatic artery. ADMB was administered in group B via the left marginal ear vein. In group C, the microbubble-contrast solution without doxorubicin was administered via the proper hepatic artery under the same conditions as group A. Group D received a mixture of 1 mg of doxorubicin in 3 ml of contrast media via the proper hepatic artery. All the injections for groups A, B, C, and D were administered at a rate of 1 ml/minute for 3 minutes, using the infusion pump for an accurate and homogenous infusion.

For the IA delivery, an 18-gauge catheter (BD Angiocath Plus with intravenous catheter, Becton-Dickinson, South Korea) was inserted into the right central auricular artery for arterial access. To reach the proper hepatic artery, a 2.0-Fr microcatheter (Progreat; Terumo, Tokyo, Japan) was advanced via the catheter into the descending aorta [21, 24]. After performing hepatic arteriography to confirm tumor staining and following visualization of the proper hepatic artery, the microcatheter was advanced selectively until the catheter tip was gently positioned at the proximal portion of the proper hepatic artery. The solution prepared for each group was then administered using an infusion pump (Genie plus, Kent Scientific Corporation) through the microcatheter at a rate of 1

ml/minute for 3 minutes, to avoid reflux of the injected complex from the proper hepatic artery [21, 25]. To access the systemic venous system, an 18-gauge catheter was inserted into the left marginal ear vein. The pressure line was then connected to catheter, and the solution was infused similarly. When the solution was completely injected, the microcatheter was removed, and the puncture site was compressed carefully to achieve hemostasis.

Ultrasound and microbubble activation

The abdominal hairs of the rabbits were carefully removed just prior to ultrasonography. The ultrasonography was performed by a radiologist both before and during drug administration in groups A, B, C, and D, using the Aplio 500 ultrasonographic system (Toshiba Medical Systems, Otawara, Japan), with 674 BT with a 8 MHz center frequency convex transducer. A fundamental B-mode ultrasound (a dynamic range of 65; a mechanical index of 1.5; a gain of 90; and a depth of 4 cm) was used to detect the VX2 tumors. After localization and a morphological examination of the tumor, the optimal plane was determined, and the skin was marked. The vascular recognition imaging mode with a low MI of 0.06 was used to detect signals generated by the microbubbles. As soon as an IA or IV delivery of the mixture through the infusion pump began, the vascular recognition mode was used to confirm the presence of tumor enhancement. Simultaneously, using a continuous up-and-down sweeping of the probe at the skin marking site, the B-mode was used to irradiate ultrasound energy to the tumor for 3 minutes (J.H.L). After cessation of infusion, additional ultrasound irradiation was applied

for 5 minutes for activating the microbubbles, resulting in a total of 8 minutes of bubble activation for each rabbit using the B-mode ultrasound.

Imaging analysis

A radiologist who was blind to the information regarding the experimental group evaluated the MR images on a picture archiving and communications system workstation. The T2-weighted images were used to confirm tumor formation and to measure the maximal longitudinal diameter (length) and maximal transverse diameter (width) of the tumors. Tumor volume was calculated from the measurements determined by MR imaging, using the modified ellipsoidal formula, tumor volume = 1/2(length × width2) [22, 26]. The volume inhibition rate (VIR) of tumor growth was calculated using the formula IR = (Tc–Tt)/Tc × 100%, where Tc represented the tumor volume of group E (control group) and Tt represents the tumor volume of each treatment group. The value of the Apparent Diffusion Coefficient (ADC) was measured quantitatively using the largest cross-section of the tumor visualized on the ADC map. The changes in the ADC values before and after TACE were evaluated.

Pathological analysis

On day 7, all animals were pre-anesthetized and sacrificed with an intravenous injection of xylazine hydrochloride, and the whole tumor was harvested after follow-up imaging. Each tumor was fixed in 10% buffered formalin. The specimen was then embedded in paraffin, cut into 4-μm sections, and the largest cross-section of the tumor was stained

with hematoxylin and eosin for basic histopathological examinations. The section was consecutively treated with terminal deoxynucleotidyl transferase dUTP nick end labeling (TUNEL) staining (ApopTag® Peroxidase in situ Apoptosis Detection Kit, Merck KGaA, Darmstadt, Germany) for evaluating tumor viability. After digital images of the histology slides were obtained (Leica Microsystems, Mannheim, Germany), the viable tumor percentage per tumor was calculated using image analysis software (Image J, version 1.45s; National Institutes of Health, Bethesda, MD, USA). In brief, the viable portion of each TUNEL stained image of the whole tumor was compared to the H&E-stained images and manually annotated by an experienced radiologist who was blind to all experimental data, in order to ensure concordance. The estimated viable tumor volume after treatment was calculated as follows: calculated tumor volume on day 7 × viable percentage of the tumor.

Biochemical liver toxicity assessment

Blood samples for assessing liver toxicity were gathered at baseline and at 1-, 3-, and 7-day intervals after treatment. Liver function tests included the assessment of liver enzymes (aspartate transaminase [AST] and alanine transaminase [ALT]).

Preparation of ADMB complex in Lipiodol for chemoembolization

To form the ADMB complex in Lipiodol, the ADMB complex at a doxorubicin concentration of 6.25/mL (aqueous phase) was dispersed in a Lipiodol (oil phase). An emulsion formulation was prepared by mixing the aqueous phase and oil phase at a ratio

of 1:2 using a vortex machine at least 5 times for 5 s. The DOX in Lipiodol group (conventional TACE formulation) is formed via 3-way pumping method.

In vitro release of doxorubicin from the ADMB complex in Lipiodol

The *in vitro* release rate of DOX were conducted on two formulations; DOX in Lipiodol and ADMB complex in Lipiodol with or without ultrasound irradiation to determine the effect of ultrasound irradiation on the *in vitro* release rate of doxorubicin. Each group was loaded into the dialysis membrane (Spectra/Por® 7, MWCO: 2 kD) and placed into the tube filled with 10 mL PBS. Dialysis membranes were maintained at a constant temperature of 37 °C in a shaking incubator at 500 rpm. The released doxorubicin was measured by high-performance liquid chromatography (HPLC). The mobile phase consisted of acetonitrile: distilled water in 50: 50 ratio with phosphoric acid 0.6 mL/L and sodium dodecyl sulfate 1.327 g/L.

Ultrasound imaging of the emulsion formulation of DOX-NPs-MB complex in Lipiodol

Conventional ultrasound imaging equipment (IU-22, Philips Medical System, Philips, Bothell, WA, USA) was used to determine whether the microbubbles in ADMB complex have ability as a contrast agent. (mechanical index: 0.06). Ultrasonic shocks were also applied four times through flash buttons installed in the instrument program (Mechanical index: 0.15) to confirm the cavitation of MB under ultrasound irradiation.

Intravascular infusion morphology of the emulsion formulation of DOX-NPs-MB complex in Lipiodol

The emulsion size of DOX-NPs-MB complex in Lipiodol emulsion formulation is larger than the diameter of capillaries in the tumor. Hence, a microfluidic channel was fabricated to identify the behavior of intra-arterially infused DOX-NPs-MB complex in Lipiodol present in peripheral capillaries of the tumor. First, the microfluidic channels mimicking blood capillary vessels were fabricated in the following steps: (1) designing the microfluidic channel map using CAD software, (2) fabricating a semiconductor-based photomask (request Nepco in Gyeonggi-do, Korea) with the CAD map; (3) making silicon wafers on which a microfluidic channel map is installed (request Amed in Seoul, Korea); (4) pouring the PDMS solution (Polydimethylsiloxane : Curing Agent = 10:1) on the surface of silicon wafer and on the glass; (5) incubating the silicon wafer in an oven at 120 °C for 12 h; (6) attaching the –OH functional group onto the surface of the two molds; (7) attaching the two molds through a dehydration condensation reaction. The emulsion formulation of DOX-NPs-MB complex in Lipiodol was infused into the microfluidic channel using a 1 mL syringe. The fluorescence of DOX-NPs was imaged to confirm how the DOX-NPs-MB complex in Lipiodol formulation exists in narrow microfluidic channels.

Visualization of the intra-arterially infused emulsion of DOX-NPs-MB complex in Lipiodol using an IVMV (in vivo micro-visualization) imaging system

To visualize liver tissue from rabbit VX2 liver tumors, a custom-built video-rate laser-scanning confocal microscopy system was used (20-22). Three continuous-wave laser modules with output wavelengths at 488 nm (MLD488, Cobolt), 561 nm (Jive, Cobolt),

and 640 nm (MLD640, Cobolt) were used as excitation light sources. Two-dimensional laser-scanning pattern was achieved by using a rapidly rotating polygonal mirror with 36 facets (MC-5, Lincoln Laser) for fast-axis scanning, and a galvanometer scanning mirror (6230H, Cambridge Technology) for y-axis scanning. The multi-color fluorescence signals were captured by a high NA commercial objective lens (CFI Plan Apo λ, 10X, NA0.45, Nikon; UPLSAP0, 4X, NA 0.16, Olympus), and detected by three photomultiplier tubes (PMT; R9110, Hamamatsu). The output signals of each PMT were digitally acquired by frame grabber (Solios, Matrox), and images were recorded and displayed with custom-written imaging software based on the Matrox Imaging Library (MIL9, Matrox) and Visual C++ (23).

Tissue optical clearing method for liver tumor samples

Samples fixed in 4 % PFA (PFA; BPP-9016, T&I, diluted in PBS) were washed with phosphate-buffered saline (PBS; LB004-02, Welgene) for 1 min. The samples were sectioned to a thickness of 300 – 500 μm and dehydrated with 80 % (wt/vol) ethanol (EtOH CAS 64-17-5; 4022-4100, Daejung) for 1 day at room temperature (RT) in a shaker. For optical clearing, dehydrated samples were immersed in peroxide-free BABB solution for 1 day at RT in a shaker. Peroxide-free BABB solution was made by mixing 40 mL of 1:2 (vol:vol) ratio of benzyl alcohol (402834, Sigma) and benzyl benzoate (B6630-1L, Sigma) with 10 g of aluminum oxide (Al_2O_3; 199443, Sigma), and after centrifuging the mixed solvents, removing the supernatant.

Animal grouping and drug delivery

The animals were randomly divided into 4 groups having similar tumor volumes: animals receiving an intra-arterial (IA) infusion of doxorubicin solution in Lipiodol (DOX in Lipiodol group, n=7)), doxorubicin encapsulating nanoparticles-microbubble complex in Lipiodol with ultrasound irradiation (DOX-NPs-MB complex in Lipiodol (US+), n=7), doxorubicin encapsulating nanoparticles-microbubble complex in Lipiodol without ultrasound irradiation (DOX-NPs-MB complex in Lipiodol (US-), n=7), and the untreated control (n=6). The dose of doxorubicin delivered at liver tumor tissue was 0.5 mg for all groups except for the control. Detailed procedure and microbubble activation using ultrasound were basically the same as the previous experiment. However, to ensure sufficient bubble activation irradiation time of ultrasonic energy was changed to 15 minutes. Imaging, pathology, liver toxicity analysis was performed in the same manner as in the previous experiment.

Visualization of the penetration of DOX-NPs into the tumor using high-content screening (HCS)

To determine the penetration efficacy of DOX-NPs into tumor tissue with or without ultrasound irradiation in the group infused with ADMB complex in Lipiodol formulation, the emulsion containing Alexa 647-NHS dye conjugated nanoparticles was injected into the VX2 tumor via the common hepatic artery. Cryo-section slides were made with tumor tissue (tissue fixed with 4 % PFA (PFA; BPP-9016, T&I, diluted in PBS). Fluorescent

imagery of the slide samples was obtained through the Operetta CLS High-Content Analysis system (Operetta CLS, PerkinElmer, Germany).

Statistical analysis

All data in the study are reported as the mean ± SD. Nonparametric analysis was conducted using the Kruskal-Wallis test to compare tumor volumes, volume inhibition rate, changes in ADC value, tumor viability, and estimated viable tumor volume in the four experimental groups. When positive results were encountered, the Mann-Whitney *post hoc* test was used for one-to-one group comparisons. Data processing and analysis were performed using the Statistical Package for the Social Sciences version 18.0 (SPSS Inc, IBM, Chicago, IL, USA). A two-sided p-value of less than 0.05 was taken to indicate that the groups differed significantly in terms of statistical results.

Results

(a)

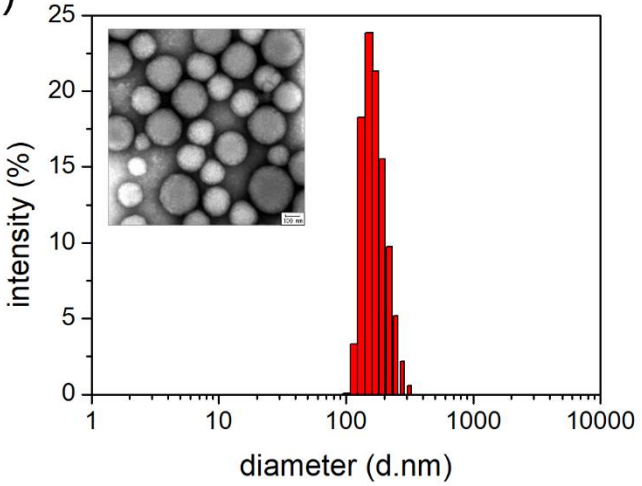
intensity (%)
diameter (d.nm)
0
5
10
15
20
25
1
10
100
1000
10000

(b)

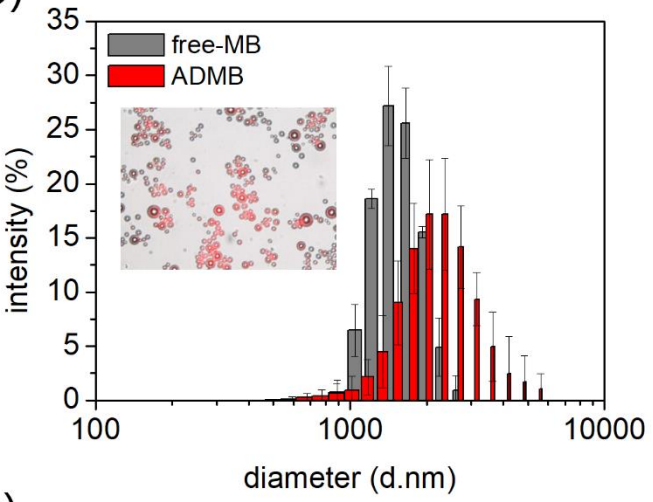
free-MB
ADMB
intensity (%)
diameter (d.nm)
0
5
10
15
20
25
30
35
100
1000
10000

(c)

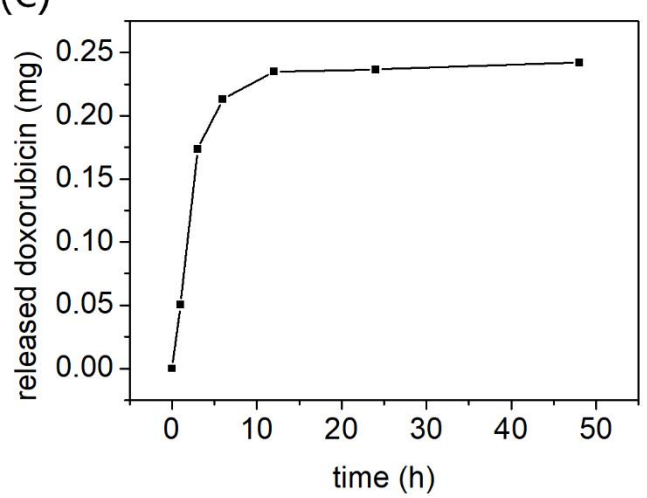
released doxorubicin (mg)
time (h)
0.00
0.05
0.10
0.15
0.20
0.25
0
10
20
30
40
50

Figure 2. Characteristics of the albumin-doxorubicin nanoparticle and the ADMB complex (a) size distribution and TEM image (inset image) of the albumin-doxorubicin nanoparticle (b) size distribution of free MB (gray) and ADMB (red). Merged fluorescence and optical images (inset image)

Preparation of the ADMB complex

The fabricated doxorubicin-albumin nanoparticles had a size distribution of 205.5 ± 45.3 nm, and transmission electron microscopic images of the albumin-doxorubicin nanoparticles demonstrated uniform and spherical morphology (Figure 2(a)). The loading efficiency of doxorubicin into the albumin-doxorubicin nanoparticle was 82.7%. The doxorubicin was released in a sustained manner from the albumin-doxorubicin nanoparticles at an in vitro release ratio of 24.2% for 50 hours with the initial burst. The phospholipid-based microbubbles were filled with the SF6 gas core and had size distributions of 1.73 ± 0.34 μm. The albumin-doxorubicin nanoparticles were conjugated onto the surface of the microbubbles and the subsequent size distribution was 2.33 ± 1.34 μm. Following albumin-doxorubicin nanoparticle conjugation, the size distribution of the ADMB complex was slightly larger in comparison to that of the free microbubble. The conjugation of the albumin-doxorubicin nanoparticles to the microbubbles was confirmed by fluorescence emission from the doxorubicin conjugated onto the surface of microbubble (Figure 2(b)).

(a)

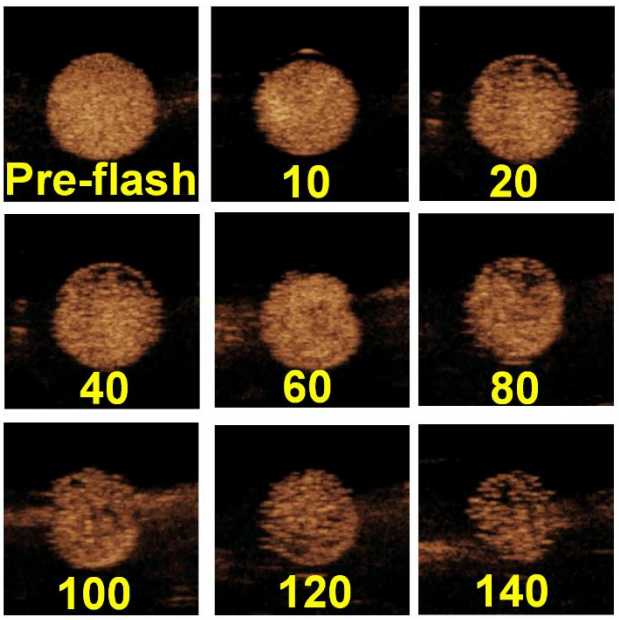
Pre-flash
10
20
40
60
80
100
120
140

(b)

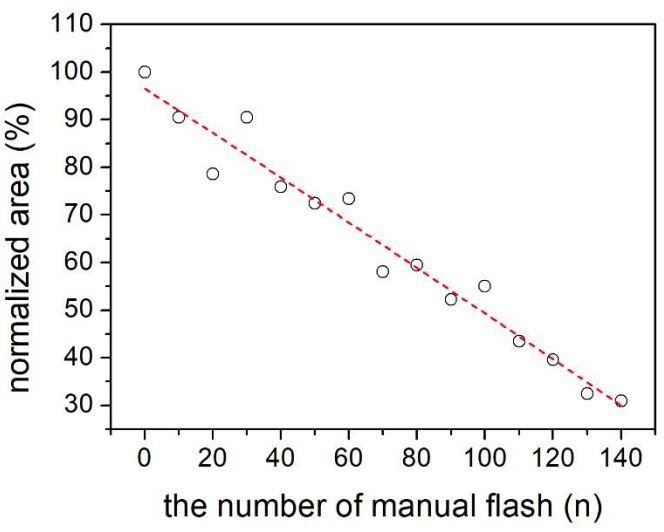
normalized area (%)
110
100
90
80
70
60
50
40
30
0
20
40
60
80
100
120
140
the number of manual flash (n)

(c)

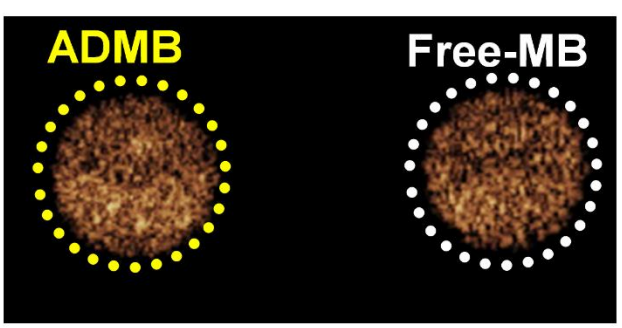
ADMB
Free-MB

Figure 3. Contrast-enhanced ultrasound images and relative quantification of ultrasound images (a) contrast-enhanced ultrasound images captured at varying numbers of manual flashes (b) relative quantification of ultrasound image (c) Ultrasound image of the ADMB complex and the free microbubble

Phantom study for echogenicity of ADMB complex

To investigate that the ADMB complex was capable of resonance to ultrasound irradiation for the cavitation effect, the echogenicity was evaluated by visualization with a clinical ultrasound scanner. For the ultrasound imaging, 2% of home-made agarose phantom containing 2-holes was used. A contrast-enhanced ultrasound imaging mode demonstrated echogenicity only from the microbubbles. At a low MI of 0.06, the ADMB complexes were stably visualized by microbubble oscillations. However, the echogenicity decreased upon microbubble destruction, depending on the number of manual flashes. Manual flashes strengthen the intensity of ultrasound exposure and lead to the destruction of the microbubbles. About 100 times of manual flashing decreased the echogenicity of the microbubbles by half (55.45%). The echogenicity consistently decreased upon increasing the number of manual flashes (Figure 3(a, b)). The differences of echogenicity between the free microbubbles and the ADMB complexes were also investigated from the ultrasound images in the same frame, to analyze whether the cavitation effect was altered by conjugation with the doxorubicin-albumin nanoparticles. The echogenicity of the ADMB complexes did not differ from the free microbubbles. The percentages of echogenic area of the ADMB complexes and the free microbubbles were 79.6% and 76.5% respectively, in equal area, relatively. (Figure 3(c)).

Animal models and ultrasound imaging during treatment procedure

The study design is summarized in Figure 4. A total of 25 VX2 liver tumor rabbit models were created. All rabbits having tumors survived through the tenure of the experiment. The tumors were visualized using ultrasound during the experiments. A strong enhancement of intra-tumoral vessels was clearly demonstrated from the beginning of the injection in the groups receiving IA microbubbles (groups A and C). Individuals receiving IV microbubbles (group B) showed a moderate tumor parenchymal enhancement as accompanied by enhanced liver parenchyma and liver vessels (Figure 5). The enhancement of ultrasound echogenicity demonstrated that the delivery efficiency of ADMB in the groups receiving IA microbubbles was higher than that of the groups receiving IV microbubbles.

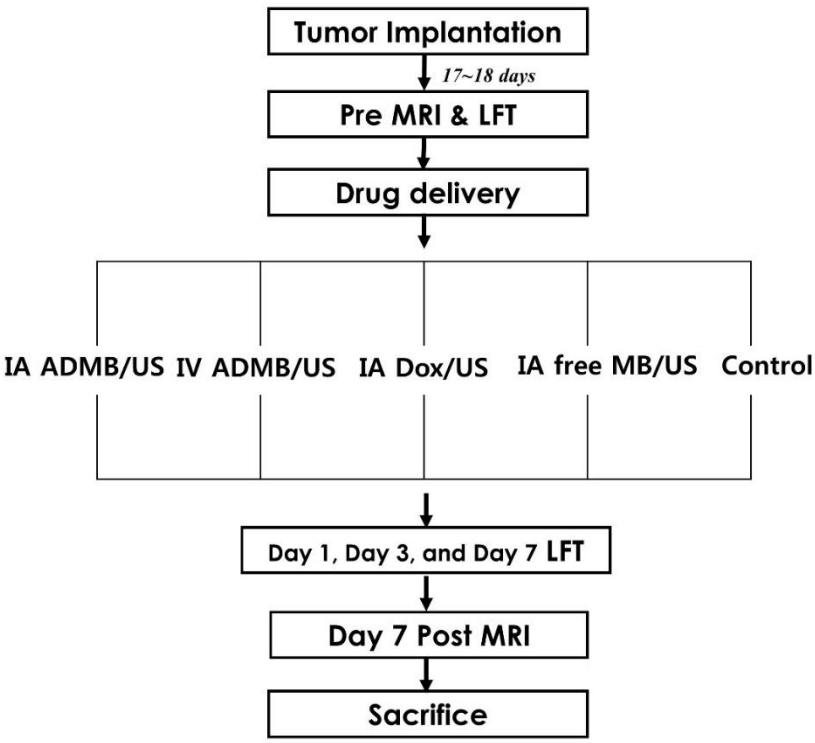

Figure 4. Study design of the VX2 rabbit liver tumor treatment protocol

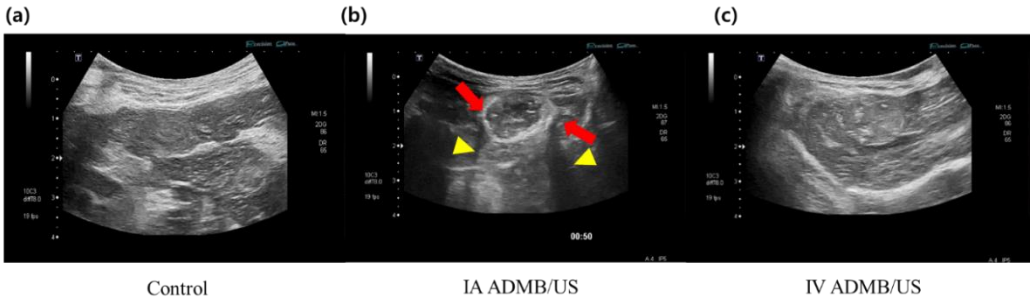

Figure 5. Representative ultrasound images of rabbit liver tumors in control (a), intra-arterial (IA ADMB/US) (b), and intra-venous (IV ADMB/US) (c) injections of albumin-doxorubicin nanoparticle-loaded microbubbles. Note the strong rim-like enhancement of intra-tumoral vessels in the periphery of the tumor (arrows) with posterior shadowing (arrowheads) in the IA ADMB/US group

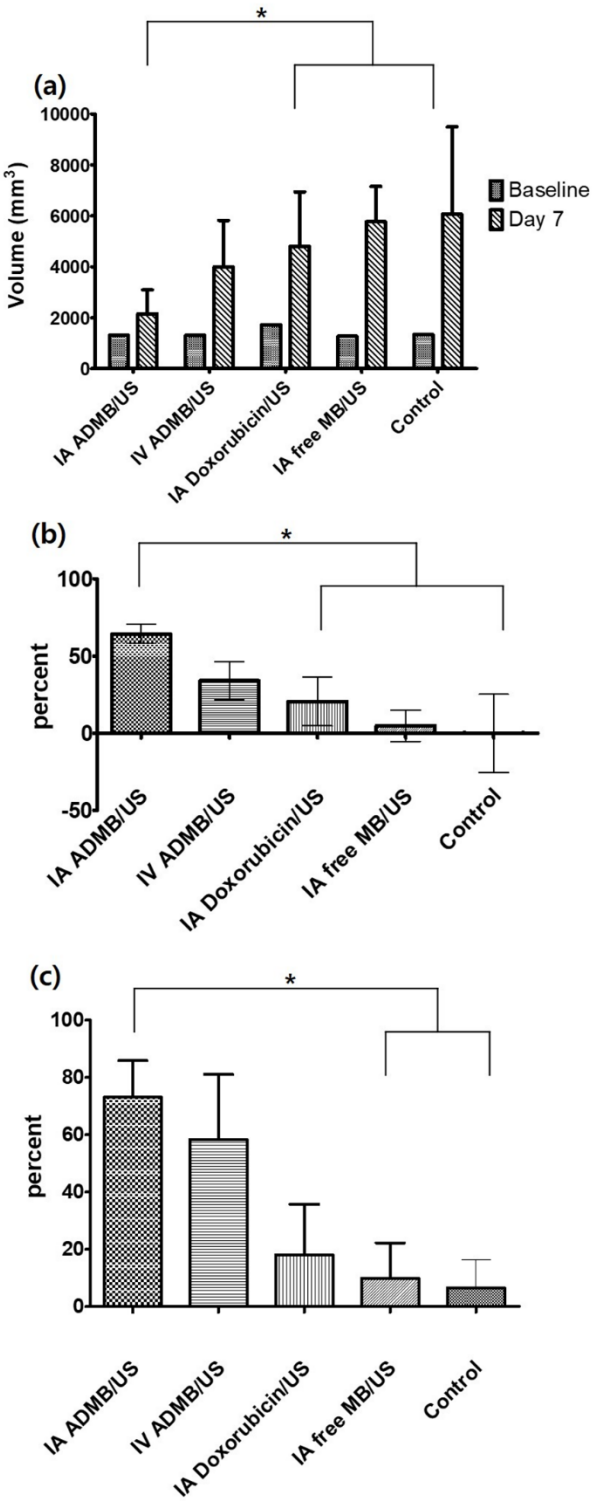
(a)
*
Volume (mm3)
10000
8000
6000
4000
2000
0
Baseline
Day 7
IA ADMB/US
IV ADMB/US
IA Doxorubicin/US
IA free MB/US
Control
(b)
*
percent
100
50
0
-50
IA ADMB/US
IV ADMB/US
IA Doxorubicin/US
IA free MB/US
Control
(c)
*
percent
100
80
60
40
20
0
IA ADMB/US
IV ADMB/US
IA Doxorubicin/US
IA free MB/US
Control

Figure 6. Quantitative volumetric image analysis at baseline and on day 7 after treatment, in IA ADMB/US, IV ADMB/US, IA Doxorubicin/US, IA free MB/US, and the untreated control groups. (a) Change in tumor volumes. (b) The Volume Inhibition Rate (VIR) of each group. (c) Percent change in ADC values across the experimental period among the groups. Each bar represents mean SD, $^{*}P < 0.05$ versus IA Doxorubicin/US, IA free MB/US, and untreated control group

Antitumor efficacy of albumin-doxorubicin nanoparticle-MB complex by quantitative MR imaging and pathology

The anticancer efficacy of ADMB was evaluated using quantitative MR imaging (Figures 6, 7(a)). The measured mean tumor volume at baseline and at 7 days after drug administration, volume inhibition rate (VIR), and change in ADC values are summarized in Figure 6. There was no significant difference in tumor size among groups at baseline ($P = 0.614$). The mean tumor volume of group A (IA ADMB/US) (2156.57 ± 849.86 mm^3) was significantly small compared to that of group C on day 7 (for groups B (IA doxorubicin alone), D (IA free MB), and E (untreated control), the values were 4811.02 ± 2132.69 mm^3, 5770.06 ± 1382.78 mm^3, and 6063.97 ± 3432.51 mm^3 respectively). The mean tumor volume of group B (IV ADMB/US) (3777.47 ± 1950.72 mm^3) was larger than that of group A, and although small in comparison to groups C, D, and E, was not statistically significant. Among the five groups, group A achieved a maximal reduction in tumor volume of $64.44 \pm 15.35\%$ on day 7 as indicated by the MRI. Both the groups A and B showed an increase in the ADC values after treatment by more than 50%, compared to pre-treatment values, which suggested the loss of diffusion-restrictive lesions such as tumor parenchyma. For group A, the VIR and percent change in ADC value were significantly higher than those of groups C, D, and E (Figure 6). In addition, the

VIR and percent change in ADC value in group B tended to be lower than the corresponding values of group A and higher than the corresponding values of groups C, D, and E; the differences, however, were not statistically significant.

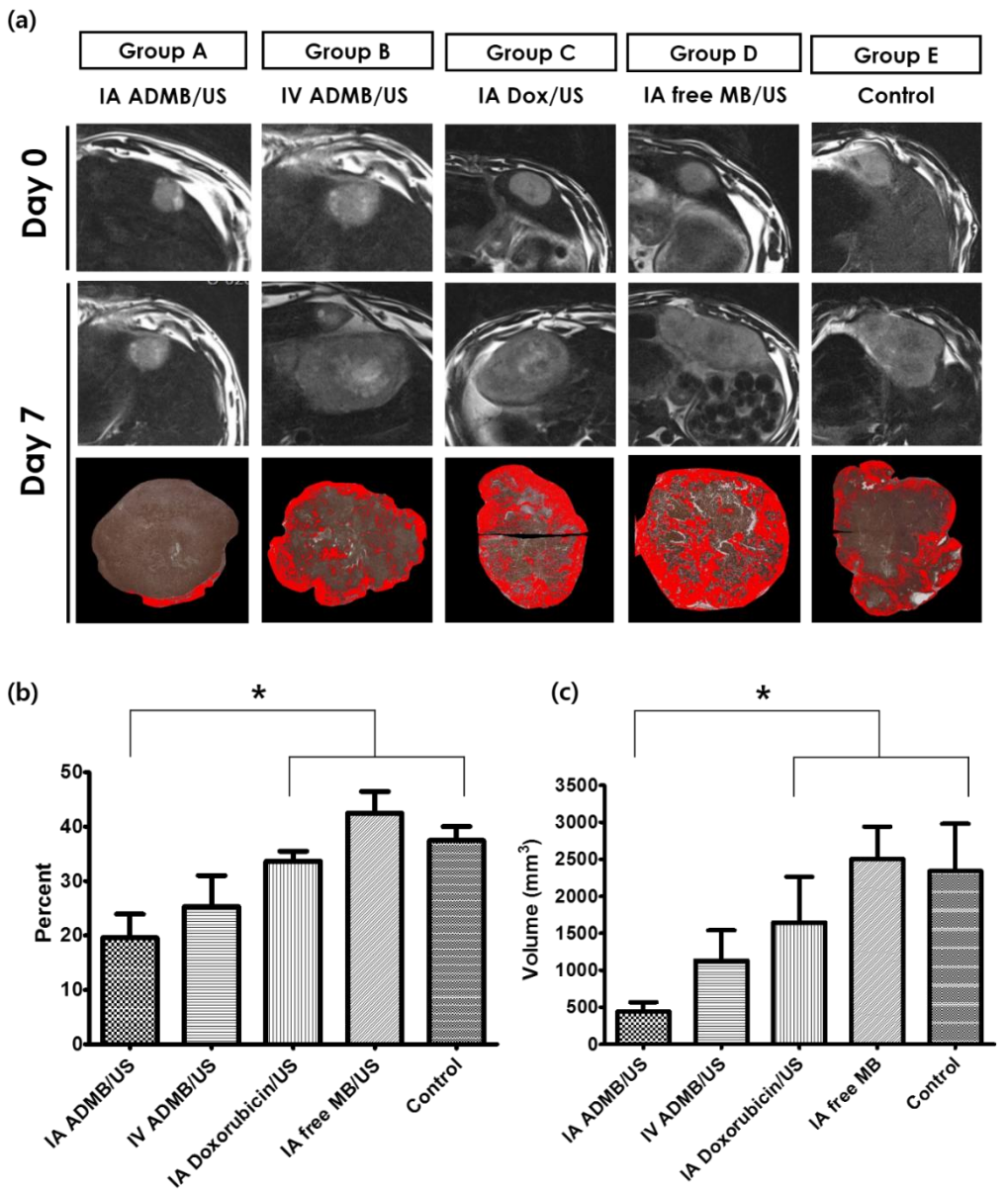

Figure 7. Representative MRI and histo-segmentation images of each group (a). Quantitative analysis of viable tumor fraction (b). Estimated viable tumor volume (c) at day 7 after treatment. Red area represents the viable portion of tumor; each bar represents mean SEM., $^{*}P < 0.05$ versus IA doxorubicin/US, IA free MB/US, and untreated control group.

The histologically viable tumor percentage was quantified using a slide-by-slide segmentation of the H&E staining images and TUNEL-stained images that were generated to investigate the entire section of the whole tumors. The pathological analysis performed on day 7 showed low viable tumors in group A (19.60±12.1%, 25.29±14.00% and 33.65±4.09%, 42.48±8.85%, 37.42±5.80% for groups A, B, C, D, and E, respectively; Figure 7(a)). Group A demonstrated a significantly higher necrotic fraction and a lower estimated viable tumor volume, compared to groups C, D, and E (Figure 7(b), 7(c)). Similar to the MR-based analysis, the viable tumor percentage and the estimated viable tumor volume of group B tended to be higher than the corresponding values of group A and lower than the corresponding values of groups C, D, and E; the difference, however, was not statistically significant.

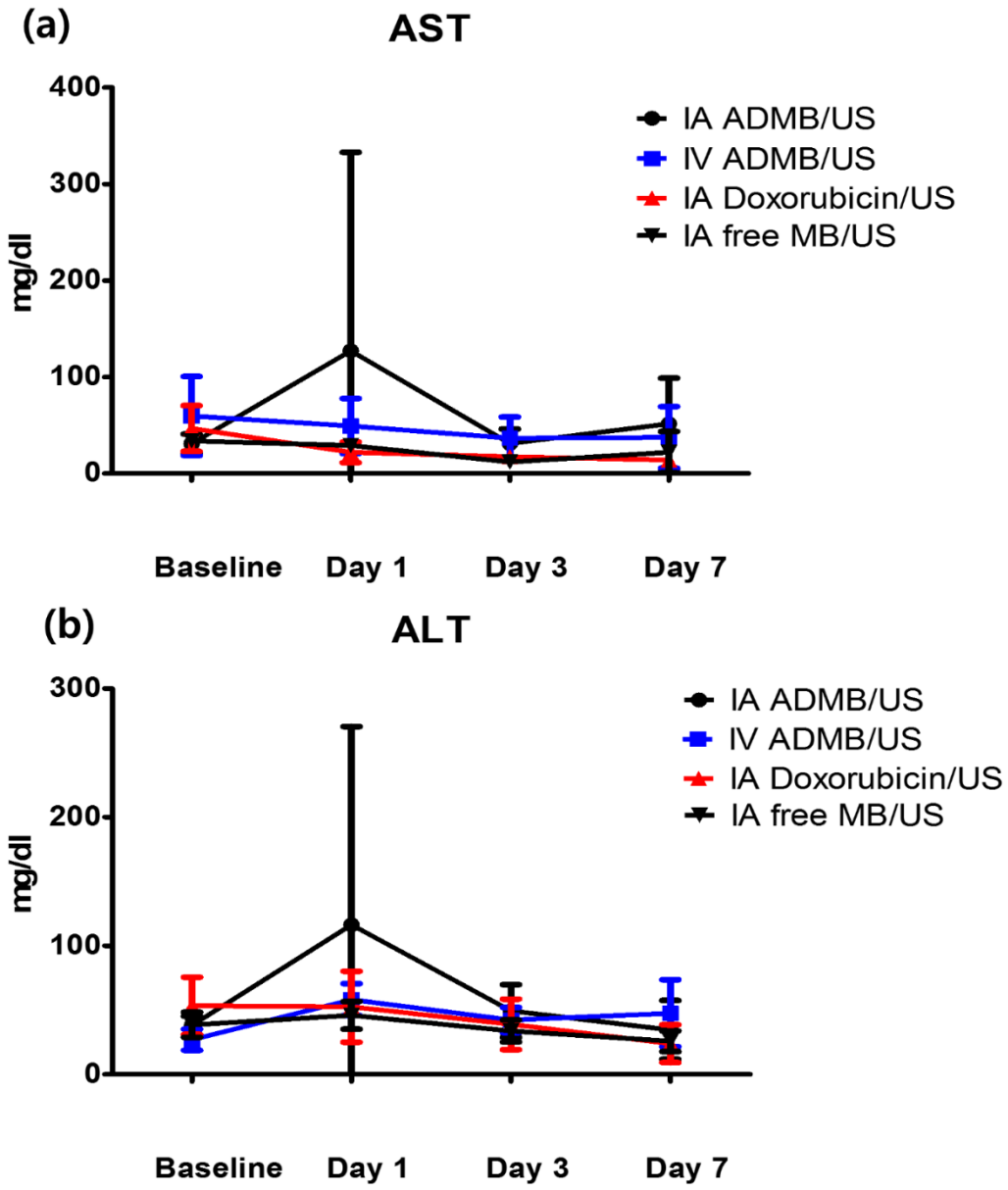

Figure 8. Graphs depicting liver enzyme values (AST, and ALT) changes over the observation period for each treatment group. (a) Graph depicting the plasma concentration changes in aspartate transaminase (AST) over the 7-day observation period (expressed in mg/dl). (b) Graph depicting the plasma concentration changes in alanine transaminase (ALT) over the 7-day observation period. No significant changes

in AST and ALT levels at each time interval throughout the observation period among the five groups

Biochemical liver toxicity evaluation

All the animals showed a tendency to reach the highest values of AST and ALT enzymes at 24 hours after treatment, which gradually decreased and returned to baseline values at 7 days after treatment. The AST and ALT values, noted at specific intervals of time starting from baseline to the end of the observation period, did not differ significantly among the five groups (Figure 8).

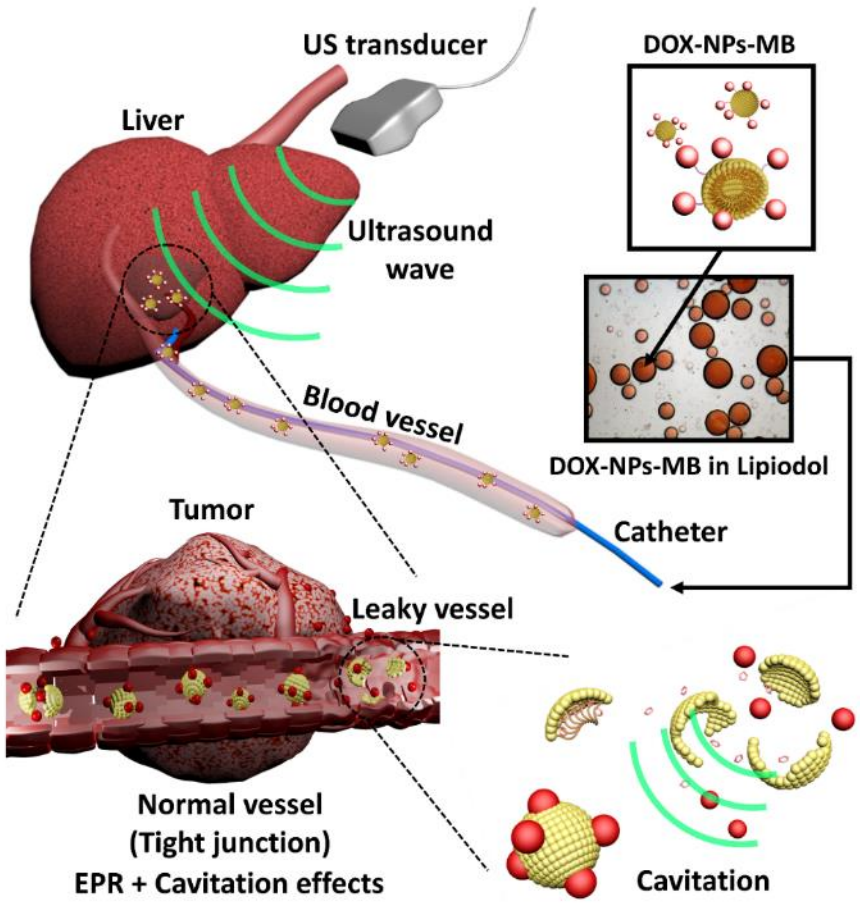

Figure 9. Schematic illustration of the part 2 study. Newly developed DOX-NPs-MB complex in Lipiodol formulation and drug delivery improvement by ultrasound irradiation (US+) during TACE procedure.

Characterization of the emulsion of ADMB complex in Lipiodol

To form the emulsion of DOX-NPs-MB complex in Lipiodol, DOX-NPs-MB complex was prepared in first step. The DOX-NPs showed a uniform size distribution, 198.30 ± 5.19 nm (Figure 10A, red color). The encapsulation efficiency of doxorubicin of DOX-

NPs was 67.2 ± 8.5 %. The size of the DOX-NPs-MB complex was determined to be 1.24 ± 0.17 μm (Figure 10A, blue color). We investigated whether the DOX-NPs-MB complex is effectively cavitated under exposure to ultrasound. The size of the DOX-NPs-MB complex after the ultrasound irradiation decreased to 225.0 ± 3.1 nm (Figure 10A, black), almost the same size as DOX-NPs, because of the effective disruption of MB. The fluorescence image in Fig. 2A demonstrates the successful conjugation of DOX-NPs onto the surface of MB by showing co-localization of DOX-NPs (green) and MB (red). The ADMB complex in contrast media (Pamiray 250, water phase) was emulsified in Lipiodol to develop a new TACE formulation. The emulsion size of DOX in Lipiodol, a conventional formulation used in the clinic (cTACE), was 37.3 ± 12.7 μm (Figure 10B, red). In comparison, the size of emulsion of ADMB complex in Lipiodol was found to be 17.7 ± 6.8 μm, being relatively smaller in size than that of DOX in Lipiodol formulation. DIC images of DOX in Lipiodol and DOX-NPs-MB complex in Lipiodol demonstrated uniform and stable emulsion morphology (Figure 10B, left images). Fluorescence images in Figure 2B reveal that both DOX in Lipiodol and DOX-NPs-MB complex in Lipiodol contained the doxorubicin chemotherapeutic agent (red) in emulsion droplets. In addition, the DIC images of DOX-NPs-MB complex in Lipiodol emulsion formulation were obtained in different time points (Figure S1), demonstrating that the emulsion of DOX-NPs-MB complex in Lipiodol remains stable for more than 1hr.

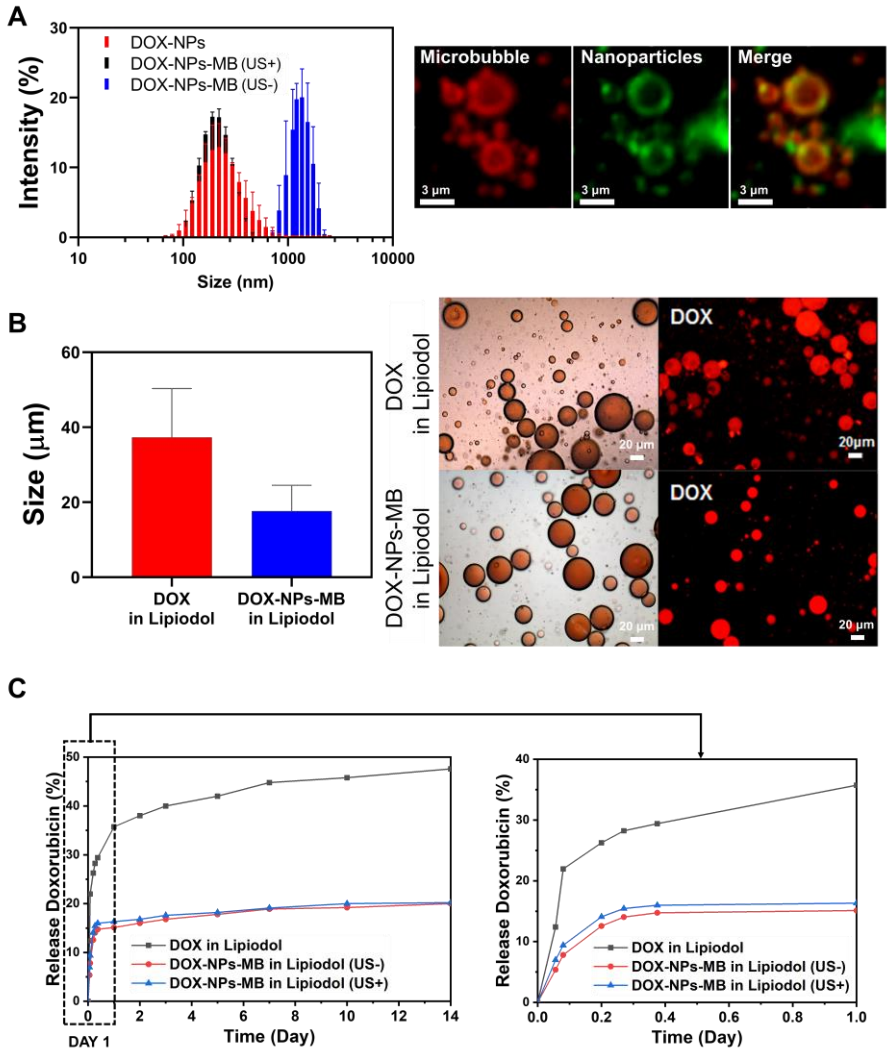

Figure 10. Characterization of the emulsion of DOX-NPs-MB complex in Lipiodol. (A) Size distribution of the DOX-NPs and DOX-NPs-MB complex with (US+) and without (US-) ultrasound and fluorescence images demonstrating the successful conjugation of DOX-NPs onto the surface of MB. (B) Size analysis of emulsion droplets in the formulation of DOX in Lipiodol and DOX-NPs-MB complex in Lipiodol (left). DIC and fluorescence images demonstrate the emulsion droplet morphology of DOX in Lipiodol and DOX-NPs-MB in Lipiodol formulations (right). (C) *In vitro* release rate of doxorubicin from the following three groups: DOX in Lipiodol, DOX-NPs-MB complex

in Lipiodol without ultrasound irradiation (US-), and DOX-NPs-MB complex in Lipiodol with ultrasound irradiation (US+). The graph shows doxorubicin release profile of each group for 14 days (left) and 1 day (right).

In vitro release of doxorubicin from the ADMB complex in Lipiodol formulation depending on ultrasound exposure

The initial doxorubicin concentration in DOX-NPs-MB complex aqueous solution was made to be 6.25 mg/mL. After the complex in aqueous solution was emulsified in Lipiodol, the doxorubicin concentration was 2.08 mg/mL (aqueous solution: Lipiodol, 1:2). *In vitro* release of doxorubicin from three groups was determined: DOX in Lipiodol, DOX-NPs-MB complex in Lipiodol without ultrasound (US-), and ADMB complex in Lipiodol with ultrasound (US+) (Figure 10C). 35.73% of encapsulated doxorubicin was released within the first 24 hours from the DOX in Lipiodol formulation, 15.11% was released within the same period from the DOX-NPs-MB complex in Lipiodol formulation without ultrasound (US-) and 16.32% was released with ultrasound (US+). There was a slight increase in doxorubicin release due to cavitation of microbubble form to US exposure, but both a sustained release of doxorubicin from the albumin nanoparticles and that ultrasound has no effect on drug release from nanoparticles.

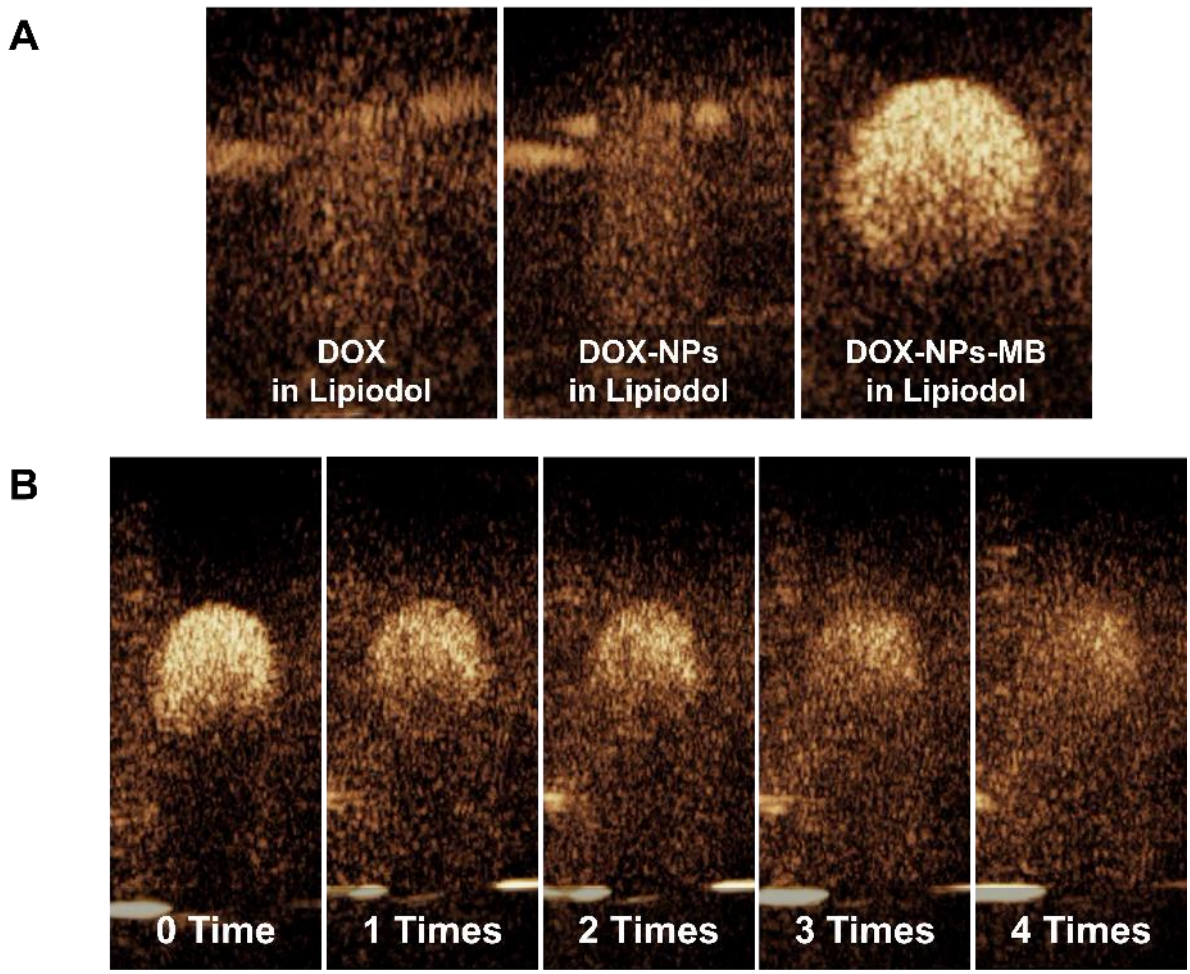

Figure 11. Ultrasound contrast intensity of DOX-NPs-MB complex in Lipiodol emulsion formulation (A) Ultrasound echogenicity of three types of formulations; DOX in Lipiodol, DOX-NPs in Lipiodol, and DOX-NPs-MB complex in Lipiodol (B) Loss of echogenicity of DOX-NPs-MB complex in Lipiodol formulation due to microbubble cavitation with increasing number of ultrasound irradiations.

Ultrasonic response of DOX-NPs-MB complex in Lipiodol emulsion formulation

The echogenicity of DOX-NPs-MB complex in Lipiodol emulsion formulation was evaluated to determine whether microbubbles in the emulsion formulation would

resonate in response to ultrasound irradiation for the real-time ultrasound imaging. The three formulations (DOX in Lipiodol, DOX-NPs in Lipiodol and ADMB in Lipiodol) were placed in holes in 2 % agarose phantom. At a low MI of 0.06, the DOX-NPs-MB complex in Lipiodol was stably visualized (Figure 11A). However, no echogenicity was found in the other groups that did not include microbubbles (DOX in Lipiodol, DOX-NPs in Lipiodol).

The effect of repeated ultrasound irradiation on echogenicity was investigated to determine if microbubbles underwent cavitation under ultrasound exposure (Figure 11B). Depending on the number of ultrasound irradiations, the echogenicity of microbubbles diminished as a result of microbubble cavitation. Although the delivery vehicle has an emulsion morphology, it can be monitored in real time with the help of the visualization of microbubbles. In addition, selective cavitation of microbubbles can be expected to improve the efficiency of drug delivery due to the sonoporation effect.

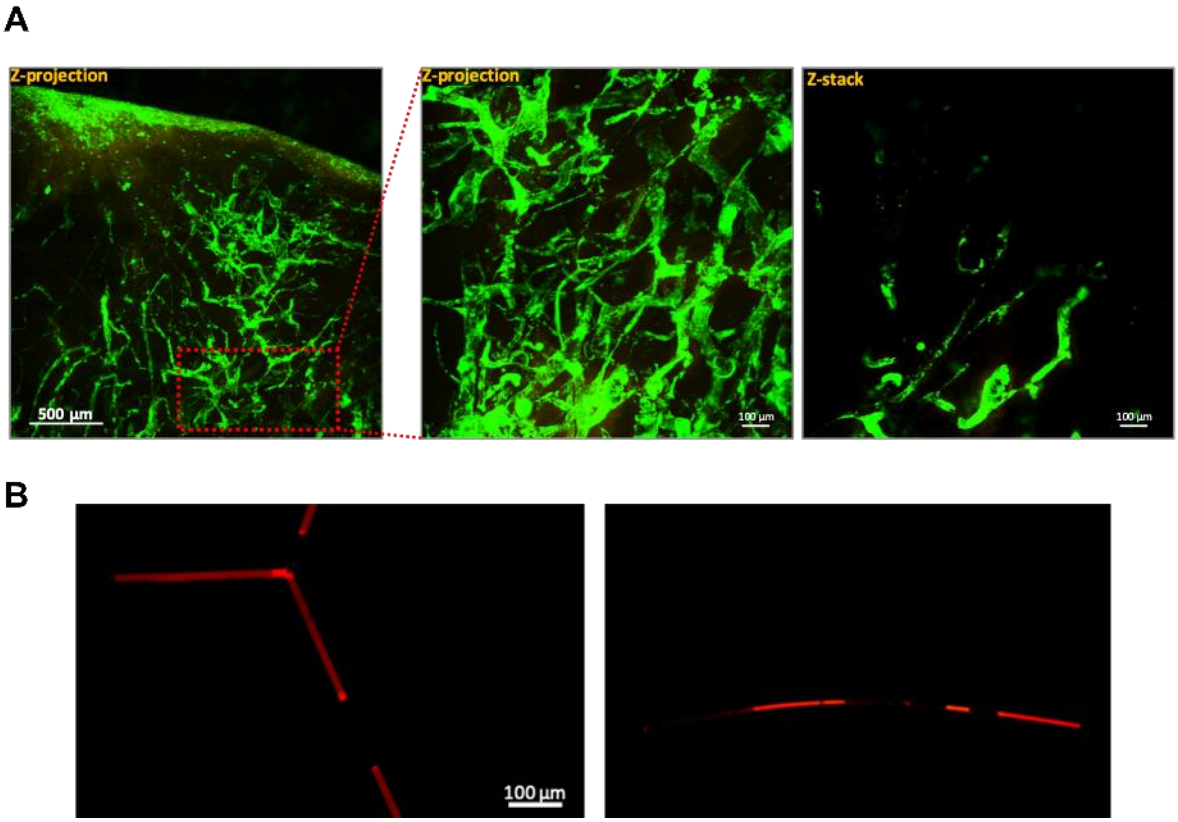

Figure 12. Intravascular distribution of the emulsion of DOX-NPs-MB complex in Lipiodol (A) Visualization of the emulsion of DOX-NPs-MB complex in Lipiodol in VX2 liver tumor using a custom-built video-rate laser-scanning confocal microscopy system (IVMV imaging system). (B) Layer-by-layer form of the emulsion of DOX-NPs-MB complex in Lipiodol in the blood vessel-like microfluidic system.

Intravascular distribution of the DOX-NPs-MB complex in Lipiodol emulsion formulation

When TACE was performed using the DOX-NPs-MB complex in Lipiodol emulsion, a custom-built video-rate laser-scanning confocal microscopy system (IVMV imaging system) was used to determine whether the developed formulation was infused into the

liver blood vessels properly. Figure 12A demonstrates the visualization of the DOX-NPs-MB complex in Lipiodol emulsion in the liver blood vessels, demonstrating that the emulsion was well infused not only into the large blood vessels, but also into the micro vessels on the surface of the liver tumor during *in vivo* experiments. The size of the DOX-NPs-MB complex in Lipiodol emulsion was approximately 17μm (Figure 10B). When the emulsion droplet is larger than the diameter of the blood vessels, it is important to evaluate how the emulsion behaves in the blood vessel. After infusion of the DOX-NPs-MB complex in Lipiodol emulsion into the blood vessel-like microfluidic system, fluorescent doxorubicin encapsulated in DOX-NPs-MB complex was observed and it was noted that the aqueous phase containing DOX-NPs-MB complex and Lipiodol exist in layer-by-layer form (Figure 12B). This suggests that the DOX-NPs-MB complex in aqueous phase is in direct contact with the blood vessel wall, rather than in the form of an emulsion in the blood micro vessels. Therefore, doxorubicin encapsulating nanoparticles (DOX-NPs) might effectively penetrate the vessel wall and be delivered into the liver tumor upon cavitation of microbubbles under the exposure of ultrasound.

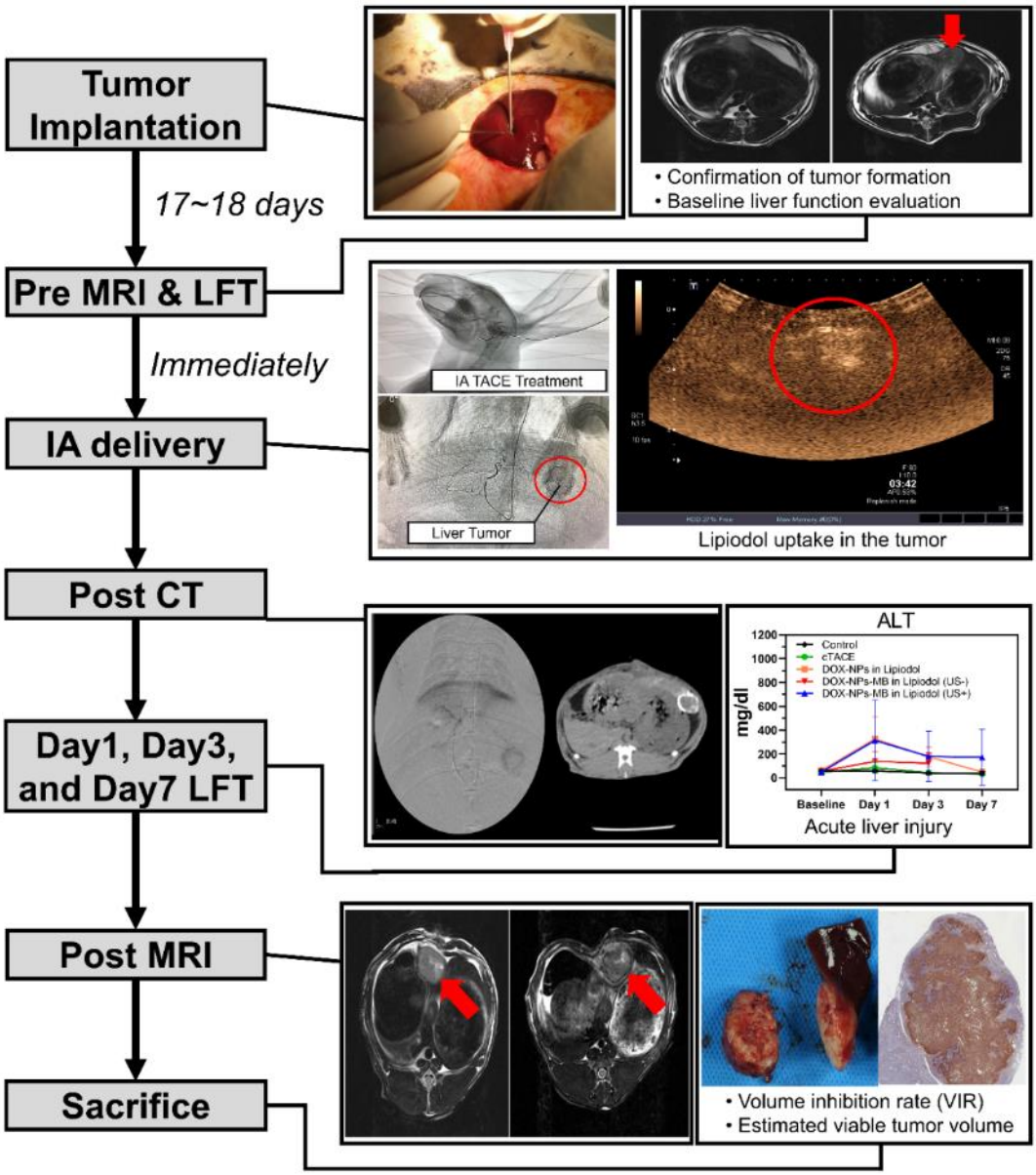

Figure 13. Experimental procedure with rabbits to verify liver cancer treatment efficacy and toxicity of DOX-NPs-MB complex in Lipiodol emulsion formulation, compared to the conventional TACE formulation.

Anticancer efficacy of DOX-NPs-MB complex in Lipiodol by quantitative MR imaging and pathology

The *in-vivo* experiment was conducted according to the procedure detailed in Figure 13. The 0.24 mL of emulsion was injected into the correct hepatic artery of the tumor-bearing rabbit. The final amount of doxorubicin delivered per rabbit should be 0.5 mg into the liver tumor, therefore, the initial concentration was set to 6.25 mg/mL. Non-contrast computed tomography (CT) scans were obtained from all animals undergoing TACE, to confirm Lipiodol uptake in the tumor area (Figure S3). The anticancer effect of DOX-NPs-MB complex in Lipiodol emulsion was evaluated by quantitative MR and histopathologic analysis of viable tumor (Figure 14). Based on the MRI imaging analysis, three groups that were drug treated, DOX in Lipiodol, DOX-NPs-MB complex in Lipiodol (US-) and DOX-NPs-MB in Lipiodol (US+), showed significantly smaller tumor sizes than the control group (Figure 14A, left). The DOX-NPs-MB complex in Lipiodol (US+) group showed the smallest tumor size on average; however, the results did not show any statistical difference between the three groups ($p > 0.05$) (Figure 14A, right). According to the histopathologic analysis of viable tumor (Figure S4), the DOX-NPs-MB complex in Lipiodol (US+) group demonstrated lowest viable portion of tumor on pathology, compared to the rest of the groups ($p < 0.05$) (Figure 14B). There was no statistical difference in viable portion of tumor between the DOX in Lipiodol treated group and the DOX-NPs-MB complex in Lipiodol (US-) treated group ($p=0.382$). On the other hand, the DOX-NPs-MB complex in Lipiodol (US+) treated group showed statistically smaller viable tumor values compared to the DOX in Lipiodol treated group

($p<0.05$). Figure 14B shows results from measurements of the volume of viable tumor. The DOX-NPs-MB complex in Lipiodol (US+) treated group showed the smallest viable tumor volume ($p < 0.05$). Differences in treatment effects between the DOX-NPs-MB complex in Lipiodol (US+) group and the DOX-NPs-MB complex in Lipiodol (US-) group indicate that the DOX-NPs-MB complex in Lipiodol emulsion are cavitated by ultrasound irradiation and results in improved permeability of the hepatic tumor vessels, and at the same time, the doxorubicin encapsulating nanoparticles are effectively delivered to the hepatic tumor. Figure 14C shows the distribution of viable tumor cells in hepatic tumors by TUNEL assay of hepatic tumor fragments in each group. Both the DOX in Lipiodol and DOX-NPs-MB complex in Lipiodol (US-) treated groups showed viable tumor cells in the peripheral and interstitial side of the tumor, whereas DOX-NPs-MB complex in Lipiodol (US +) treated group demonstrated tumor cells were consistently apoptotic expired, including in the peripheral portion of the tumor (Figure 6C). Considering that cancer recurrence is caused by residual cancer cells remaining in the peripheral region of the tumor, the results of TUNEL assay (Figure S5) demonstrates the possibility of effective cancer recurrence prevention, by delivering chemotherapeutic agent effectively by ultrasound irradiation and killing cancer cells in the peripheral region. In order to confirm the cavitation effect of microbubbles on the delivery of chemotherapeutic agent encapsulating nanoparticles into the hepatic tumor, the distribution of fluorescently conjugated nanoparticles with or without ultrasound irradiation was determined by HCS analysis (Figure 15). Relatively more particles can

be seen in the DOX-NPs-MB complex in Lipiodol (US+) treated group, indicating the sonoporation effect of microbubbles on the delivery of nanoparticles into tumors.

Biochemical liver toxicity evaluation

All rabbits showed a tendency to reach the highest concentration values of AST and ALT enzymes in serum at 24 h after treatment, which gradually decreased and returned to baseline at 7 days after treatment. The AST and ALT values, noted at specific time intervals, did not differ significantly among the treatment groups (Figure 8). When the liver is damaged or destroyed by chemotherapeutic agents, AST and ALT in the tissue are released into the bloodstream. Therefore, levels reflect liver damage. On day 1, highest enzyme levels were seen with the DOX-NPs-MB complex in Lipiodol (US+) group, indicating that the combination of DOX-NPs-MB complex and ultrasound irradiation enhanced the efficacy of anticancer drugs. This result may suggest that the DOX-NPs-MB complex in Lipiodol (US+) treated group had a relatively large number of nanoparticles penetrating inside the tissue, compared to ultrasound negative group.

Discussion

In this study, the DOX-NPs-MB complex in Lipiodol emulsion formulation was developed as a new ultrasound triggered TACE formulation to overcome the low delivery efficiency of drugs due to rapid elimination of the anticancer drug into the systemic circulation and high side effects (24). The DOX-NPs-MB complex in Lipiodol emulsion formulation could be monitored in real-time during the TACE procedure because

microbubbles were stably present in the emulsion and resonated under exposure to ultrasound at a low MI value of 0.06 (Figure 3). During intra-arterial infusion, the cavitation of microbubbles at a high MI value of 1.5, created jet-streaming and enhanced permeability of doxorubicin encapsulated nanoparticles into the tumors. The doxorubicin would be expected to release continuously from the nanoparticles upon delivery into the tumor (25). The sustained release of chemotherapeutic agents from nanoparticles has two positive effects. First, when drug-encapsulating nanoparticles are delivered to tumors, they release the drug for an extended period of time, resulting in long-term treatment effects, and secondly, when nanoparticles leak into the systemic circulation, the exposure of highly concentrated chemotherapeutic agents into normal tissues can be prevented and side effects can be minimized. In conventional TACE, the success of the procedure can be only determined by the presence of Lipiodol uptake in the tumor seen on CT image. In contrast, the ultrasound and CT guided multidimensional real-time monitoring were feasible from the newly developed emulsion formulation, DOX-NPs-MB complex in Lipiodol (Figure 5). Multi-dimensional real-time monitoring enables accurate intra-procedural assessment of drug delivery, and the irradiation of ultrasound energy with high MI could induce sonoporation effects that enhance the delivery efficiency of chemotherapeutic nanoparticles into tumors.

Since the emulsion size of DOX-NPs-MB complex in Lipiodol was larger than diameter of micro-vessels, the newly developed emulsion formulation was confirmed to be present in the blood vessels as layers (Lipiodol oil phase – DOX-NPs-MB complex aqueous phase – Lipiodol oil phase), not as an emulsion form (Figure 4). This reveals that

DOX-NPs-MB chemotherapeutic complex is placed in the vicinity of the blood vessel wall and a sufficient sonoporation effect can be expected under exposure to ultrasound. The DOX-NPs-MB complex in Lipiodol was found to be cavitated under the exposure of ultrasound at an MI value of 1.5 (Figure 3B). The cavitation of microbubbles generated a jet-streaming, temporarily causing stress in the surrounding cell membrane, which is known as inertial cavitation (26). It generates pores between the cells constituting the tumor vascular wall and delivers doxorubicin encapsulating nanoparticles efficiently into the tumor (Figure 1). Overall, the DOX-NPs-MB complex in Lipiodol emulsion formulation (US+) showed more effective anticancer efficacy than DOX-NPs-MB complex in Lipiodol (US-). The difference in chemotherapy effect with or without ultrasound irradiation can be attributed to cavitation of microbubbles (Figure 6).

The conventional TACE formulation is an emulsion of aqueous droplets in an oil phase in which the aqueous phase containing anticancer agents and the ratio of the oil phase can be in a volume ratio of 1 to 4. However, it was not appropriate to adjust the initial doxorubicin concentration in the newly developed DOX-NPs-MB complex in Lipiodol emulsion formulation because of the low encapsulation efficiency of chemotherapeutic agent in nanoparticles. So, the DOX in Lipiodol and DOX-NPs-MB complex in Lipiodol formulations used in this study were prepared at an aqueous to oil phase ratio of 1:2 to deliver 0.50 mg of doxorubicin. The TACE formulation depends on oil to aqueous phase ratio, number of three-way pumping, and properties of anticancer drugs (27, 28). Although the oil phase component was lower than the conventional 1:4 emulsion ratio, it was confirmed that the emulsion formulation was made properly (Figure 2B). Emulsions

produced at 2:1 ratios (oil phase to aqueous phase) are known to be less stable than at 4 to 1 (29). Although the DOX-NPs-MB complex in Lipiodol was stable during the *in vivo* experiment, long-term stability will need to be evaluated.

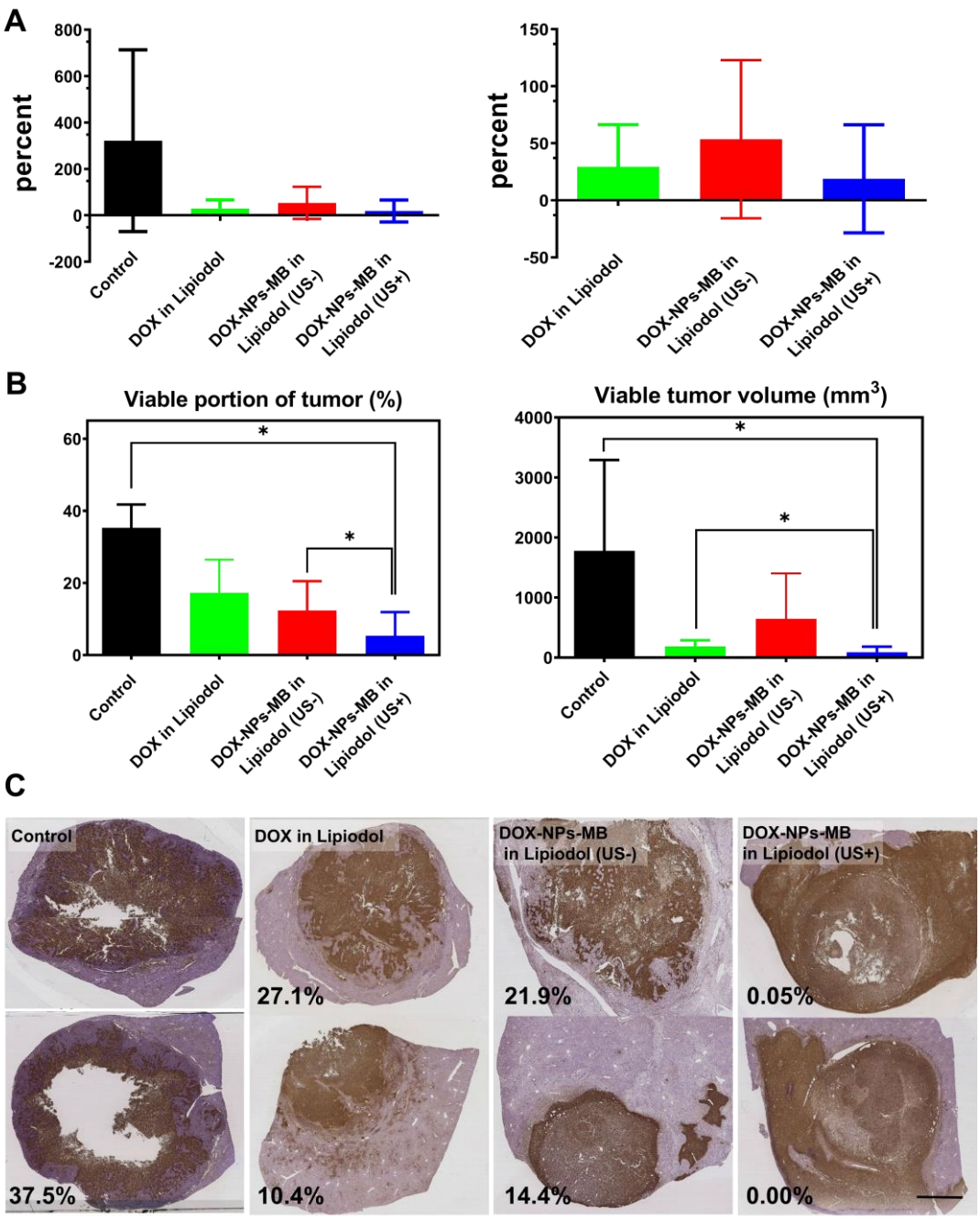

Figure 14. ***In vivo*** **therapeutic efficacy of DOX-NPs-MB complex in Lipiodol compared to the conventional TACE formulation, DOX in Lipiodol** (A) Comparison of tumor volume growth inhibition for each formulation. (B) Analysis of the proportion

of viable cancer cells in a tumor after cancer treatment with each formulation (C) Representative histo-segmentation images of each group. Quantitative analysis of viable tumor fraction. The scale bar indicates 500 μm.

In the *in-vivo* therapeutic efficacy study, there was no statistically significant difference in tumor size inhibition between the group treated with the conventional TACE formulation and with the newly developed DOX-NPs-MB complex in Lipiodol formulation (Figure 14A). However, compared with other groups, the DOX-NPs-MB formulation (US+) group showed dramatic tumoricidal effects, including in the peripheral region of the tumor on histopathologic analysis (Figure 14C and Figure S3). As follow up imaging was performed only on day 7 following the treatment, this might be insufficient to show treatment outcomes thoroughly. From the pathologic point of view, the main way to prevent the recurrence of cancer is to control the residual tumor cells in the peripheral region of tumor, where tumor cells are directly located besides healthy liver tissue and have potential to penetrate or metastasize adjacently. Thus, the TUNEL assay results of the DOX-NPs-MB complex emulsion formulation plus ultrasound group showed promising anti-cancer efficacy, in terms of the potential to effectively suppress cancer recurrence (30). The result of HCS analysis demonstrated the distribution of doxorubicin loaded nanoparticles (Figure 15). The nanoparticles were consistently located in the peripheral region of the tumor tissue where continuous release of doxorubicin, would ensure sufficient and sustained therapeutic effects could be obtained.

This study has some limitations. This study was not performed based on detailed optimization of ultrasonic properties. The optimal duration and frequency of ultrasound irradiation, as well as the level of delivered irradiation energy, must be addressed. In order to apply these experimental results to human studies, moreover, it is essential to analyze the effect of the ultrasound-DOX-NPs-MB complex interaction according to the depth of the lesion in detail as attenuation of the ultrasound effect may occur. Moreover, to apply these techniques to clinical practice, the development of dedicated device to deliver optimal ultrasound energy for activating microbubbles in the target tissue is mandatory. Another limitations is that although the VX2 liver tumor model are widely used for preclinical study for TACE, fundamental difference of histologic type from actual hepatocellular carcinoma limits direct translation of the results in clinical HCCs.

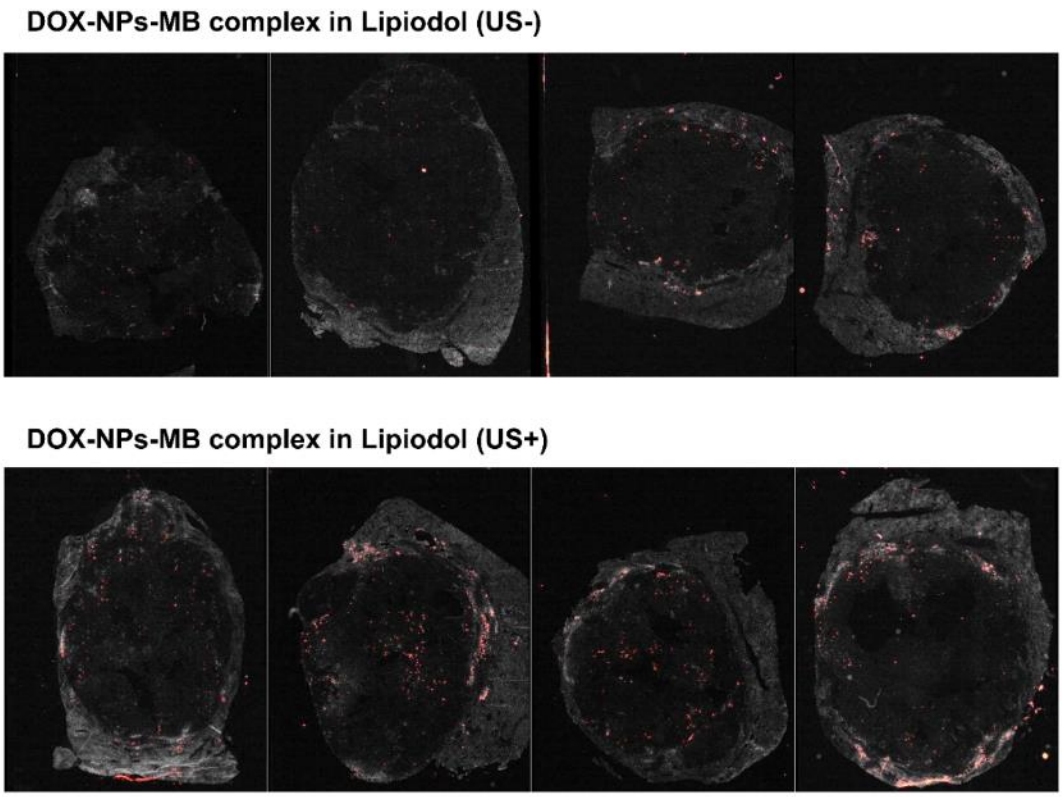

Figure 15. ***In vivo*** **HCS experimental data showing the distribution of nanoparticles in liver tumor with or without ultrasound irradiation after infusion of DOX-NPs-MB complex in Lipiodol formulation**. Red spots indicate the distribution of nanoparticles in the hepatic tumors.

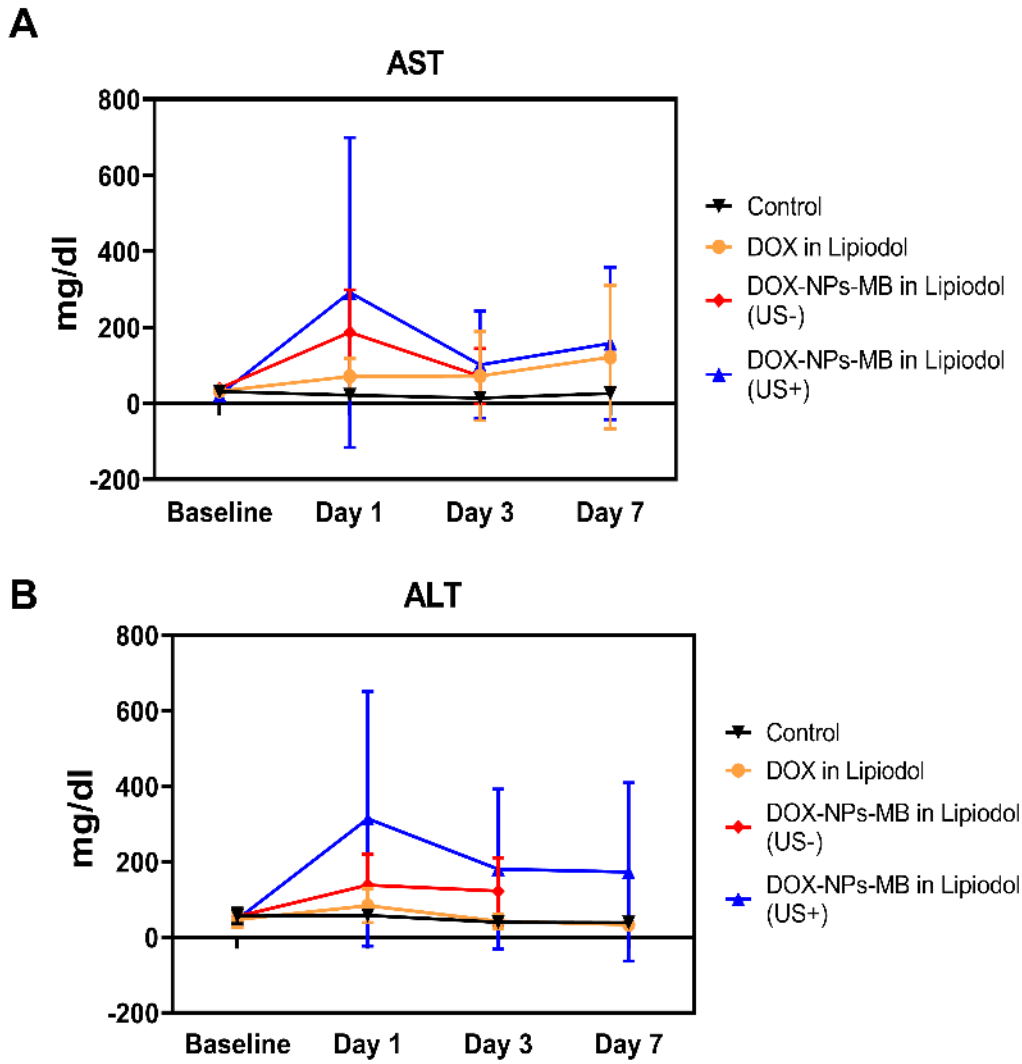

Figure 16. Biochemical liver toxicity evaluation The (A) AST and (B) ALT values for 7 days after treatment with each formulation; DOX in Lipiodol, DOX-NPs-MB complex in Lipiodol (US-), DOX-NPs-MB complex in Lipiodol (US+).

Conclusion

To overcome the disadvantages of conventional TACE formulations and to maximize treatment efficacy, we developed a DOX-NPs-MB complex in Lipiodol emulsion formulation in this study. Microbubbles, an ultrasound contrast agent in the formulation allowed for real-time imaging of the TACE procedure with ultrasound, during the infusion of DOX-NPs-MB complex in Lipiodol emulsion into feed vessels of a tumor. In addition, ultrasound of high mechanical index was focused on the tumor and the sonoporation effect induced by cavitation of microbubbles effectively delivered nanoparticles carrying chemotherapeutic agents into tumors, resulting in improved treatment efficacy compared to conventional TACE. The new concept of ultrasound sensitive TACE formulation developed in this study is expected to be a new paradigm for the treatment of liver cancer.

References

1. Willatt J, Hannawa KK, Ruma JA, Frankel TL, Owen D, Barman PM. Image-guided therapies in the treatment of hepatocellular carcinoma: A multidisciplinary perspective. World journal of hepatology 2015;7(2):235.

2. Bruix J, Sala M, Llovet JM. Chemoembolization for hepatocellular carcinoma. Gastroenterology 2004;127(5):S179-S188.

3. Gaba RC, Emmadi R, Parvinian A, Casadaban LC. Correlation of doxorubicin delivery and tumor necrosis after drug-eluting bead transarterial chemoembolization of rabbit VX2 liver tumors. Radiology 2016;280(3):752-761.

4. European Association for the Study of the Liver. Electronic address eee, European Association for the Study of the L. EASL Clinical Practice Guidelines: Management of hepatocellular carcinoma. Journal of hepatology 2018;69(1):182-236. doi: 10.1016/j.jhep.2018.03.019

5. Llovet JM, Bruix J. Systematic review of randomized trials for unresectable hepatocellular carcinoma: chemoembolization improves survival. Hepatology 2003;37(2):429-442.

6. Choi JW, Cho H-J, Park J-H, Baek SY, Chung JW, Kim D-D, Kim H-C. Comparison of drug release and pharmacokinetics after transarterial chemoembolization using diverse lipiodol emulsions and drug-eluting beads. PloS one 2014;9(12):e115898.

7. Nakakuma K, Tashiro S, Hiraoka T, Uemura K, Konno T, Miyauchi Y, Yokoyama I. Studies on anticancer treatment with an oily anticancer drug injected into the ligated feeding hepatic artery for liver cancer. Cancer 1983;52(12):2193-2200.

8. Ueno K, Miyazono N, Inoue H, Nishida H, Kanetsuki I, Nakajo M. Transcatheter arterial chemoembolization therapy using iodized oil for patients with unresectable hepatocellular carcinoma: evaluation of three kinds of regimens

and analysis of prognostic factors. Cancer 2000;88(7):1574-1581.
9. Wu J, Nyborg WL. Ultrasound, cavitation bubbles and their interaction with cells. Advanced drug delivery reviews 2008;60(10):1103-1116.
10. Lu Q, Liang HD, Partridge T, Blomley MJ. Microbubble ultrasound improves the efficiency of gene transduction in skeletal muscle in vivo with reduced tissue damage. Gene Ther 2003;10(5):396.
11. Church CC, Carstensen EL. “Stable” inertial cavitation. Ultrasound in medicine & biology 2001;27(10):1435-1437.
12. Wischhusen J, Padilla F. Ultrasound-targeted microbubble destruction (UTMD) for localized drug delivery into tumor tissue. IRBM 2018.
13. Kudo N, Okada K, Yamamoto K. Sonoporation by single-shot pulsed ultrasound with microbubbles adjacent to cells. Biophysical journal 2009;96(12):4866-4876.
14. Kooiman K, Foppen-Harteveld M, van der Steen AF, de Jong N. Sonoporation of endothelial cells by vibrating targeted microbubbles. Journal of controlled release 2011;154(1):35-41.
15. Moon H, Yoon C, Lee TW, Ha KS, Chang JH, Song TK, Kim K, Kim H. Therapeutic Ultrasound Contrast Agents for the Enhancement of Tumor Diagnosis and Tumor Therapy. J Biomed Nanotechnol 2015;11(7):1183-1192.
16. Han H, Lee H, Kim K, Kim H. Effect of high intensity focused ultrasound (HIFU) in conjunction with a nanomedicines-microbubble complex for enhanced drug delivery. Journal of controlled release : official journal of the Controlled Release Society 2017;266:75-86. doi: 10.1016/j.jconrel.2017.09.022
17. Elzoghby AO, Samy WM, Elgindy NA. Albumin-based nanoparticles as potential controlled release drug delivery systems. Journal of controlled release 2012;157(2):168-182.
18. Weber C, Coester C, Kreuter J, Langer K. Desolvation process and surface

characterisation of protein nanoparticles. International journal of pharmaceutics 2000;194(1):91-102.
19. Lee JH, Moon H, Han H, Lee IJ, Kim D, Lee HJ, Ha S-W, Kim H, Chung JW. Antitumor Effects of Intra-Arterial Delivery of Albumin-Doxorubicin Nanoparticle Conjugated Microbubbles Combined with Ultrasound-Targeted Microbubble Activation on VX2 Rabbit Liver Tumors. Cancers 2019;11(4):581.
20. Song E, Seo H, Choe K, Hwang Y, Ahn J, Ahn S, Kim P. Optical clearing based cellular-level 3D visualization of intact lymph node cortex. Biomedical optics express 2015;6(10):4154-4164.
21. Seo H, Hwang Y, Choe K, Kim P. In vivo quantitation of injected circulating tumor cells from great saphenous vein based on video-rate confocal microscopy. Biomedical optics express 2015;6(6):2158-2167.
22. Choe K, Hwang Y, Seo H, Kim P. In vivo high spatiotemporal resolution visualization of circulating T lymphocytes in high endothelial venules of lymph nodes. Journal of biomedical optics 2013;18(3):036005.
23. Acar M, Kocherlakota KS, Murphy MM, Peyer JG, Oguro H, Inra CN, Jaiyeola C, Zhao Z, Luby-Phelps K, Morrison SJ. Deep imaging of bone marrow shows non-dividing stem cells are mainly perisinusoidal. Nature 2015;526(7571):126.
24. Dhanasekaran R, Kooby DA, Staley CA, Kauh JS, Khanna V, Kim HS. Comparison of conventional transarterial chemoembolization (TACE) and chemoembolization with doxorubicin drug eluting beads (DEB) for unresectable hepatocelluar carcinoma (HCC). Journal of surgical oncology 2010;101(6):476-480.
25. Moon H, Yoon C, Lee TW, Ha K-S, Chang JH, Song T-K, Kim K, Kim H. Therapeutic ultrasound contrast agents for the enhancement of tumor diagnosis and tumor therapy. Journal of biomedical nanotechnology 2015;11(7):1183-1192.

26. Prentice P, Cuschieri A, Dholakia K, Prausnitz M, Campbell P. Membrane disruption by optically controlled microbubble cavitation. Nature physics 2005;1(2):107.
27. Deschamps F, Moine L, Isoardo T, Tselikas L, Paci A, Mir L, Huang N, Fattal E, de Baere T. Parameters for stable water-in-oil lipiodol emulsion for liver trans-arterial chemo-eembolization. Cardiovascular and interventional radiology 2017;40(12):1927-1932.
28. Masada T, Tanaka T, Nishiofuku H, Fukuoka Y, Sato T, Tatsumoto S, Marugami N, Kichikawa K. Techniques to form a suitable lipiodol-epirubicin emulsion by using 3-way stopcock methods in transarterial chemoembolization for liver tumor. Journal of Vascular and Interventional Radiology 2017;28(10):1461-1466.
29. He M-K, Zou R-H, Wei W, Shen J-X, Zhao M, Zhang Y-F, Lin X-J, Zhang Y-J, Guo R-P, Shi M. Comparison of stable and unstable ethiodized oil emulsions for transarterial chemoembolization of hepatocellular carcinoma: results of a single-center double-blind prospective randomized controlled trial. Journal of Vascular and Interventional Radiology 2018;29(8):1068-1077. e1062.
30. Shimada M, Hasegawa H, Gion T, Shirabe K, Taguchi K-i, Takenaka K, Tanaka S, Sugimachi K. Risk factors of the recurrence of hepatocellular carcinoma originating from residual cancer cells after hepatectomy. Hepato-gastroenterology 1999;46(28):2469-2475.

국문 초록

서론: 경동맥화학색전술 (Transarterial chemoembolization; TACE)는 간암의 국소 치료에서 중요한 위치를 차지하고 있는 치료법이다. 그러나 고식적인 TACE 는 주입한 에멀젼이 불안정하여 혈액 내에서 빠르게 분리되면서 국소 약물 전달 효과는 떨어지고 전신 부작용이 생기는 문제점이 있다. 본 연구는, 이와 같은 TACE 의 한계를 극복하기 위한 초음파 감응형 항암제 함유 알부민 나노입자-마이크로버블 복합체와, 이 복합체와 요오드화 기름과의 새로운 에멀젼을 개발하여 약물전달능 및 종양살상능을 향상시키는 새로운 초음파 감응형 간동맥화학색전술용 에멀젼을 개발하는 것이다.

방법: 이 연구는 크게 2 단계로 구분되어 있다. 먼저 항암제 함유 나노입자-마이크로버블 복합체 (Albumin nanoparticle-Doxorubicin conjugated Microbubble; ADMB) 를 제작하고 물리화학적 특성 을 분석하였다. In-vivo study 를 위하여 토끼 VX2 간종양 모델을 이용하였다. 최종적으로 개발된 ADMB 와 iodized oil 과의 에멀젼을 이용하여 in-vitro characteristics 및 in-vivo therapeutic efficacy 와 safety 를 검증하였다.

결과: ADMB 는 약 2.33 ± 1.34 μm 의 크기를 가지며 doxorubicin loading efficiency 는 82.7%였다. ADMB 는 2-9 MHz 주파수 범위에서 가시적인 초음파 조영능을 보였으며 방사하는 초음파 세기에 따라 cavitation 효과를

보였다. 토끼 간종양 모델을 이용한 실험에서 ADMB 군은 치료를 하지 않은 대조군에 비해 약 5 배의 종양 성장 억제 효과를 보였다.

DOX-NPs-MB 에멀젼 역시 ADMB 와 유사한 정도의 초음파 조영능을 보였고 in-vivo 실험에서 새로 개발된 DOX-NPs-MB 에멀젼을 외부 초음파와 감응시키면서 종양에 주입하였을 때, 기존 에멀젼보다 유의하게 높은 종양 살상능을 보였고 간독성에는 두 군간 차이가 없었다.

결론: 새로 개발된 외부 초음파 감응형 DOX-NPs-MB 에멀젼은 기존의 고식적인 에멀젼보다 약물 전달능, 종양 살상능이 우수하였으며 초음파로 실시간 약물 전달 모니터링이 가능하였다. 이 새 에멀젼은 TACE 에서 간암 치료 효과를 높일 수 있는 새로운 수단이 될 것으로 기대된다.

주요어: 경동맥화학색전술, 초음파, 마이크로버블, Sonoporation, Theragnostics, 나노의학, 간세포암

학 번: 2010-21816